Artificial Neural Network-Based Modeling of Liquid Membranes for Separation of Cerium (III)

A dissertation

submitted in partial fulfillment of the requirements for the award of the degree

of

MASTER OF SCIENCE

in

CHEMISTRY

Submitted by:

Urooj Fatima (2K24/MSCCHE/61)

Under the supervision of

Dr Manish Jain

DEPARTMENT OF APPLIED CHEMISTRY
DELHI TECHNOLOGICAL UNIVERSITY
(Formerly Delhi College of Engineering)
Bawana Road, Delhi – 110042

JUNE 2026

DELHI TECHNOLOGICAL UNIVERSITY
(Formerly Delhi College of Engineering)
Shahbad Daulatpur, Main Bawana Road, Delhi-42

CANDIDATE'S DECLARATION

I, Urooj Fatima (2k24/MSCCHE/61) the students of M.Sc. Chemistry, hereby certify that the work which is being presented in the dissertation entitled **"Artificial Neural Network-Based Modeling of Liquid Membranes for separation of Cerium (III)"** in partial fulfillment of the requirements for the award of the degree of Master of Science in Chemistry, submitted in the Department of Applied Chemistry, Delhi Technological University, is an authentic record of my own work carried out during the period from 2025 to 2026 under the supervision of Dr. Manish Jain.

The matter presented in the thesis has not been submitted by me for the award of any other degree of this or any other Institute.

Place: Delhi
Date: 22/06/2026

Urooj Fatima
(2k24/MSCCHE/61)

DELHI TECHNOLOGICAL UNIVERSITY

(Formerly Delhi College of Engineering)
Shahbad Daulatpur, Main Bawana Road, Delhi-42

CERTIFICATE

This is to certify that Urooj Fatima (2K24/MSCCHE/61) has carried out this research work presented in this project report entitled **"Artificial Neural Network-Based Modeling of Liquid Membranes for separation of Cerium (III)"** for the award of Degree of Master of Science in Chemistry from Department of Applied Chemistry, Delhi Technological University, Delhi, under my supervision. The dissertation embodies the results of original work, and studies are carried out by the student herself, and the content of the thesis do not form the basis of the award of any other degree to the candidate or to any other body else from this or any other University/Institution.

Place: Delhi **Dr Manish Jain**

Date: 22/06/2026 **(SUPERVISOR)**

ACKNOWLEDGEMENT

The success and final outcome of this project required a lot of guidance and assistance from many people and we are extremely fortunate to have got this all along the completion of this project work.

I wish to express our deepest gratitude to our project supervisor, Dr. Manish Jain, Department of Applied Chemistry, Delhi Technological University. His scholastic guidance, sagacious suggestions, and ongoing encouragement helped me in completing this project within time frame.

I wish to thank Prof. D. Kumar, Head of the Department of Applied Chemistry, Delhi Technological University for his constant motivation.
I am thankful and fortunate enough to get constant encouragement, support and guidance from all teaching staff of Department of Applied Chemistry, which helped me in successfully completing my project work.

Finally, yet importantly, I would like to express my heartfelt thanks to my beloved family and friends who have endured my long working hours and whose motivation kept me going.

UROOJ FATIMA

ABSTRACT

The rare earth elements (REEs) have been used in a range of applications from permanent magnets to catalysts, optical devices, electronic materials and many others, with remarkable quantities. The rare earth metal cerium (Ce) is widely used, however, because it is easily accessible in the industry. One of the methods which is promising to replace the conventional methods for separation and recovery of cerium from dilute aqueous solution is Emulsion Liquid Membrane (ELM) due to its high selectivity, low consumption of solvent, extraction-stripping process and high mass transfer efficiency. The process of extraction of Ce (III) ions was predicted and investigated in the present work by ANN modeling technique with ELM as carrier extractant, Span 80 as surfactant, Kerosene as diluent and HNO3 as stripping agent.

The extraction time, pH of feed phase, concentration of the feed, and the concentration of the surfactant, stripping phase, stirring speed, phase ratio, treatment ratio and initial cerium concentration were used as input variables in this analysis.

Feed forward multi-layer perceptron (ANN) was used to describe the effect of the process parameter to the extraction performance and the Levenberg-Marquardt back propagation algorithm was used for the training of the ANN. Five statistical measures MSE, Pearson correlation coefficient (R), RMSE, MAE and RPE were used to assess the model's predictive ability. The optimized 9–11–1 ANN model achieved overall $R = 0.99082$ ($R^2 = 0.9817$) and $MSE = 26.145$ ($RMSE \approx 5.11\%$). The sensitivity analysis shows that the biggest sensitivity is with the pH (28%) and the concentration of D2EHPA (23%).

The obtained values obtained from the modelling were in good agreement with the experimental ones and the extraction behavior of Ce (III) was very accurate. This indicates that the modeling based on ANN is well suitable for the modeling of ELM for rare earth elements recovery.

The keywords used are: Rare Earth Elements, Cerium, Emulsion Liquid Membrane, Artificial Neural Network, D2EHPA, Extraction Efficiency, Modeling and Optimization.

CONTENT

LIST OF ABBREVIATIONS

ANN	–	Artificial Neural Network
REE	–	Rare Earth Element
ELM	–	Emulsion Liquid Membrane
SLM	–	Supported Liquid Membrane
BLM	–	Bulk Liquid Membrane
D2EHPA	–	Di-(2-Ethylhexyl) Phosphoric Acid
HNO_3	–	Nitric Acid
MLP	–	Multilayer Perceptron
MSE	–	Mean Squared Error
R	–	Correlation Coefficient
LM	–	Levenberg–Marquardt
Ce	–	Cerium
Nd	–	Neodymium
Dy	–	Dysprosium
La	–	Lanthanum
PVDF	–	Polyvinylidene Fluoride
RO	–	Reverse Osmosis
MAP	–	Modified Atmosphere Packaging
DOE	–	Design of Experiments
W/O/W	–	Water/Oil/Water Emulsion
REEs	–	Rare Earth Elements
rpm	–	Revolutions per Minute

LIST OF TABLES

LIST OF FIGURES

CHAPTER 1: INTRODUCTION

1.1 INTROUCTION TO RARE EARTH ELEMENTS

The Rare Earth Elements (REEs) are a group of seventeen elements which include fifteen lanthanide elements, as well as scandium and yttrium elements (Ni'am et al., 2020; Ronda et al., 1998). The 4f electronic orbital are filled in a step-by-step manner, which results in very similar chemical and physical properties among these elements. Although 'rare' it does not imply that some are as rare as they are said to be in the earth's crust. However, they do not accumulate in amounts large enough for mining and it will be challenging to separate them due to their similarities.

Not only essential materials in high tech application today but are also in great demand (REEs), Due to their excellent magnetic, luminescent and catalytic properties (Ni'am et al., 2020; Ronda et al., 1998), they are considered for use in wind turbines, electric vehicle batteries, defense and medical devices, etc. There has been a dramatic increase in the demand for the rare earth elements, especially in the context of electric vehicles, wind power, consumer electronics and clean energy technology across the world (Ni'am et al., 2020; Ronda et al., 1998). The need for creative solutions to deal with the efficient recovery, purification and separation of these metals has come with the surge. Rare Earth (REE) recovery has been reduced in impacts compared to the older hydrometallurgical methods which are more expensive and is playing an increasing role in the world economy more and more. Of these, the membrane-based separation technique (especially liquid membrane technology) has a very high selectivity, low chemical consumption and low energy consumption (Kujawa et al., 2023a).

1.2 CERIUM AND ITS INDUSTRIAL IMPORTANCE

The largest and most abundant REE in the Lanthanide family is cerium (Ce). The oxidation states of cerium, Ce (III) and Ce (IV) are extraordinary. Cerium has a wide range of applications, especially in the production of products. Because of its superior abrasive properties, cerium oxide is used as a polish. Cerium is an important component in catalytic converters used in the automobile industry, used to promote oxidation and reduction reactions. Fluorescents, making phosphors, solar, optoelectronics, fuel cells, and ceramics are all applications of cerium compounds.

In recent years, cerium has been used in the field of clean energy technology. It has many applications including batteries and hydrogen storage as well as renewable energy. With an increase in usage of cerium compounds in different applications, there has been a rise in cerium-containing industrial wastes.

A significant amount of cerium ions is present in aqueous solutions in waste water associated with the mining process, metallurgy, e-waste recycling process and manufacturing of catalysts. This waste material lowers the pollution of the environment and is an example of how the resources can be used in the extraction of cerium. Due to the high cost and increasing usage in industry, researches have focused on developing effective and selective Ce (III) extraction processes from dilute aqueous solutions.(Kujawa et al., 2023b, 2023a)

1.3 OBJECTIVES OF THE PRESENT WORK

The prime goal of the present thesis is to build a model using Artificial Neural Network (ANN) technique to predict the efficiency of extraction of Ce (III) ions from aqueous solution by Emulsion Liquid Membrane (ELM) method. Hence, the present study aims at investigating the relationship between the important operating variables and Ce (III) extraction efficiency.

- Firstly, this research work aims to explore the composition of the emulsion liquid membrane (ELM) system for the extraction of Ce (III) which involves both external feed phase containing Ce (III) and organic membrane phase (D2EHPA and Span 80 in kerosene) and internal stripping phase (HNO3).
- The second purpose is to determine key process parameters that influence the transport of Ce (III) in ELM system, which are extraction time, feed phase pH, concentration of D2EHPA, concentration of Span80, concentration of HNO_3, stirring speed, ITM, treatment ratio and initial Ce (III) concentration.
- The third goal is to build the feed-forward artificial neural network model which can predict the extraction efficiency of Ce (III) with the process variables obtained above. For this, a multilayer perceptron (MLP) network will be used because it has a capability to model nonlinear chemical or separation processes.
- The fourth objective is to assess the predictive ability of the ANN model by computing some statistical parameters including correlation coefficient and mean square error, and to determine the optimal architecture of the network with the maximum predictive accuracy and the minimum prediction error.
- The fifth goal is to study the effect and interaction of operational parameters on the efficiency of the extraction of Ce (III) using the ANN model and obtain the optimum operating parameters for maximum efficiency of Ce (III) extraction.

CHAPTER 2: LITERATURE REVIEW

2.1 CONVENTIONAL SEPARATION TECHNIQUES FOR Ce (III)

Various traditional approaches have been used for the separation and recovery of cerium ions from aqueous solutions. These methods include chemical precipitation, ion exchange, adsorption and solvent extraction. All these methods have demonstrated their effectiveness in specific situations, but have drawbacks that prohibit their use for large-scale applications.

One of the earliest methods used for the extraction of metal ions is chemical precipitation (Allahkarami & Rezai, 2021). The precipitants such as oxalates, carbonates and hydroxides are added to the solution containing cerium compounds and the compounds are precipitated. The precipitates formed by this method are recovered by the use of filtration or settling. However, this technique has its disadvantages including low selectivity, chemical waste and high sludge production.

In Ion Exchange, synthetic resins containing functional groups, which exchange ions with metal species in solution are used(Allahkarami & Rezai, 2021) .The cerium ions are absorbed on resin surface, and then recovered by ion exchange methods. Ion exchange method is highly selective but is coupled with the high cost of resin material, regeneration and complex solution chemistry conditions.

The use of adsorption has been shown to be promising due to its simplicity of operation and versatility [7]. Various adsorbents such as activated carbon (AC), zeolites, metal oxides, biochar and functionalized polymers (FP) have been investigated as candidate adsorbents for rare earth ions (REIs). But adsorption technique may have low adsorption capability, poor mass transfer and adsorbents regeneration problems.

The current process for the separation of rare earth elements is called conventional process, where the solvent extraction process is dominant(Kamil et al., 2019). The most commonly used extractants for selective extraction of lanthanide ions are D2EHPA, Cyanex272, Cyanex921, and EHEHPA (Kamil et al., 2019; Randhawa et al., 2016). While solvent extraction is highly efficient and highly selective for rare earth element separation, it has several drawbacks such as multiple stage extraction and stripping process, losses of solvent, high volume of solvents and operation costs.

Thus, there is a need to develop membrane-based separation methods, which can effectively combine high selectivity with less chemical consumption and energy.

2.2 LIQUID MEMBRANE TECHNOLOGY

The liquid membrane technology has been proposed as one of the most promising alternative separation and recovery process of metal ions from aqueous solution to the conventional solvent extraction process (Perkins et al., 2007; Randhawa et al., 2016). This is because the technology is based on the extraction properties of solvent extraction, and selective transport properties of membrane processes in a single unit operation. Liquid membrane has several advantages such as low consumption of solvents, high selectivity, low energy consumption, process can be space-saving, and it can be run on very low concentrations of dissolved materials.

Liquid membranes can be classified in three basic categories:

1. Bulk Liquid Membranes (BLM)
2. Supported Liquid Membranes (SLM)
3. Emulsion Liquid Membranes (ELM)

The simplest type of liquid membranes are bulk liquid membranes which are formed by a layer of liquid membrane (L) between two aqueous phases. The use of these membranes is still limited to practical use due to slow mass transfer. The supported liquid membrane (SLM) is similar to BLMs, in that a polymer support is impregnated with the organic carrier phase but with the advantage that there is a larger surface area on which the interfaces are found, which brings better kinetic properties (Mao et al., 2015; Perkins et al., 2007). The major disadvantage of SLMs is the instability due to the gradual removal of the organic phase from the porous support. Finally, ELM is the most advanced type of liquid membranes with outstanding extraction characteristics, extremely high rate of transfer and high interfacial area, hence very attractive for industrial applications. The formation of liquid membranes has opened up new possibilities in the development of technology for the recovery of rare metals in the process.

2.3 EMULSION LIQUID MEMBRANE (ELM)

The Emulsion Liquid Membrane (ELM) technique was first developed as a separation technique that could extract and strip in one step [13]. ELM is one of the most advanced liquid membrane separation techniques which has been extensively investigated due to its high mass transfer property and low energy requirement.

The ELM system is considered as a water-in-oil-in-water (W/O/W) double emulsion composed of three different phases:

- External Feed Phase
- Organic Membrane Phase
- Internal Stripping Phase

The external feed phase has the desired target metal ions which will be separated from it by using ELM. The membrane phase is a mixture of an organic solvent with carrier extractant and surfactant. The stripping step is an internal step that stores the recovered metal ions.

There are basically two stages of emulsification in the construction of an ELM system. The first step is to emulsify the internal stripping solution into the organic membrane phase to create a water in oil emulsion. In this way this emulsion is then further emulsified in the external aqueous solution to give a W/O/W emulsion system.

The efficiency of ELMs is influenced by various parameters such as feed phase pH, carrier concentration, surfactant concentration, agitation rate, stripping phase concentration, phase ratio, treatment ratio and extraction time.

Some of the main benefits of using ELM technology are:

- Combined extraction and stripping
- High enrichment factors
- Large surface area of the interface
- Small solvent requirement
- High rate of mass transfer
- High selectivity
- Effective treatment of dilute solutions

The performance of these qualities renders ELM to be a versatile technology for rare earth elements recovery, wastewater treatment, separation of different metal ions such as bismuth, copper, and rare earths, etc. (Laguel & Samar, 2024a; Mao et al., 2015)

2.4 D2EHPA AS A CARRIER EXTRACTANT

Among the acidic organophosphorus compounds, especially widely used in hydrometallurgy and in membrane separations is Di-(2-Ethylhexyl) Phosphoric Acid (D2EHPA). This selectivity for trivalent rare earth ions has resulted in a thorough study of the extraction of cerium, neodymium, dysprosium, lanthanum and others lanthanides using D2EHPA.

D2EHPA has two branched hydrocarbon chains with a phosphoric acid part. D2EHPA is a non-polar organic solvent and has the HR_2 (dimer) structure. The metal ion extraction is carried out with the reaction with the dimer $(HR)_2$ compound by cation exchange.

Based on the equilibrium reaction suggested by Taamallah et al. and verified by Hachemaoui et al. and the extraction of Ce (III) by D2EHPA can be represented as follows:

$$Ce^{3+} + 3(HR)_2 \rightleftharpoons Ce\,(HR_2)_3 + 3H^+$$

If it is deduced from this reaction, it can be said that the extraction process will be greatly affected by the concentration of hydrogen ions in the feed solution. These lower hydrogen ions will lead to the formation of complexes which will increase the transport into the membrane (Laguel & Samar, 2024b, 2024a).

D2EHPA has some characteristics as an extractant:

- Strong binding affinity towards trivalent rare earth ions
- High extraction efficiency
- Good chemical stability
- Commercial availability
- Affordability
- Reversible extraction-stripping process

The extractant has been successfully applied in solvent extraction, supported liquid membranes and emulsion liquid membranes. Some studies have shown that efficiencies close to 100% can be obtained under the best working conditions (Ahmad et al., 2022; Laguel & Samar, 2024b)

D2EHPA was selected in this work as an effective carrier extractant and was found to be suitable for ELMs with kerosene as a diluent for the membrane.

2.5 ARTIFICIAL NEURAL NETWORKS (ANN)

The Artificial Neural Network (ANN) is a model of computation modeled after the architecture of biological neural networks. ANNs are constructed in a way that enables them to learn from raw data complex nonlinear relations. From chemical engineering and separation technology point of view, ANN is found very useful for modelling, simulation, prediction, optimization and control applications.

An ANN basically comprises processing units called neurons. These neurons are structured in three basic types of layers:

- Input Layer
- Hidden Layer
- Output Layer

These layers are responsible for accepting process variables from the input layer, computing nonlinear operations in the hidden layer and predicting with respect to the process variable in the output layer. Amongst various ANN models, Feed Forward MLP (Multilayer Perceptron) has proved to be the most effective one. Feed Forward MLP network: Information flows in a feedforward fashion from the input neurons to hidden neurons, then on to output neurons.

During training process, connection weights of the network can be changed by optimization algorithms in order to decrease error. There are a number of different types of training algorithms in which Levenberg–Marquardt Backpropagation algorithm is widely recognized for its ability to converge quickly and make accurate predictions.

In this work, the extraction efficiency of Ce (III) in an ELM system has been predicted by using ANN model. The operating parameters were taken as the inputs and extraction efficiency was taken as the output variable. The ANN architecture was optimized as follows:

- Input Neurons = 9
- Hidden Layer Neurons = 11
- Output Neurons = 1

From the simulation results, it is clear that the model is quite accurate with $R > 0.99$ and MSE of 26.145. Based on the above conclusion, it can be concluded that using ANN modeling in the study of Ce (III) extraction is very promising.

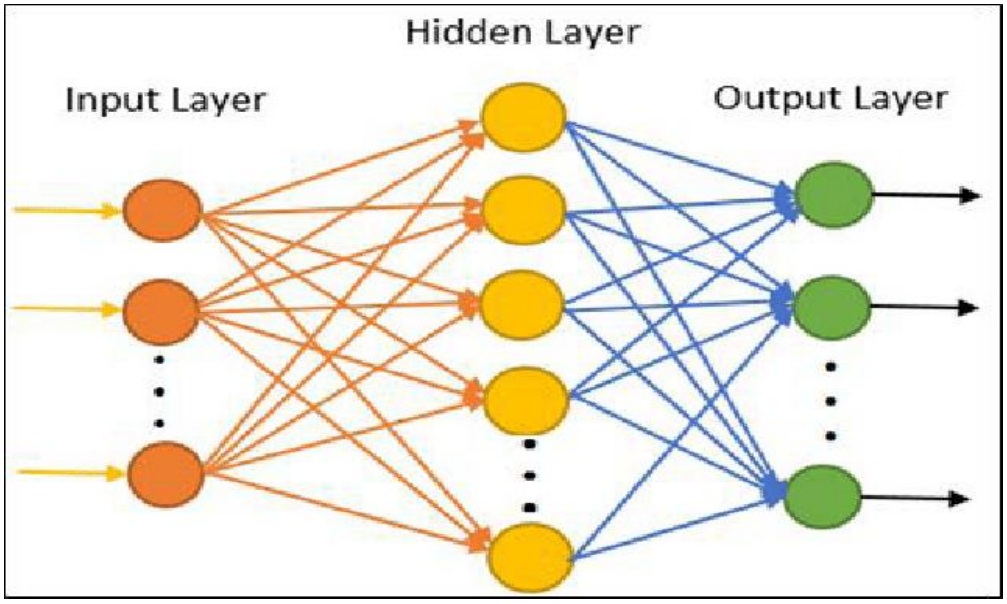

Figure 1: Architecture of Artificial Neural Network (ANN)

2.6 ANN APPLICATIONS IN MEMBRANE SEPARATION PROCESSES

- ANNs have been used successfully in numerous studies in membrane separation processes. ANN is able to describe membrane fouling, permeate flux reduction and solute rejection by considering the complex interactions between feed composition, pressure, membrane properties and the filtration time, in many cases with a superior accuracy compared to classical regression techniques in the field of nanofiltration.
- ANN has also been extensively utilized for forecasting the performance of reverse osmosis (RO) systems including permeate production, salt rejection, energy consumption, and overall performance. Through training this ANN can assist with process optimization when the interactions of variables like feed salinity, pressure, temperature, membrane age and recovery ratio are understood.
- One of the most useful applications of ANN is for the separation of rare earth elements, where the extraction efficiency and selectivity can be influenced by relatively small changes in pH, extractant concentration, and/or phase composition. It has predictive power, which means that a full knowledge of complex transport and complexation mechanisms is not necessary.
- ANN is well suited to modelling of liquid membrane extraction processes as it can model the effect of multiple influences such as chemical equilibrium, membrane diffusion, hydrodynamics, emulsion stability and extractant recovery. That is particularly true in the case of multi-phase, multi-interface emulsion liquid membrane systems.
- The Ce (III)-ELM system was used in this study to predict the extraction efficiency with the help of nine input variables by applying ANN. Because of the high nonlinearity of Ce (III) transport and the lack of a complete and reliable mechanistic model, ANN should be used. The performance of the model was very good, with the correlation coefficient greater than 0.99, and MSE of 26.145, which proves its effectiveness in modeling Ce(III) extraction.(Abu Shmeis et al., 2021)

2.7 RESEARCH GAP IDENTIFICATION

Several separation methods exist for the separation of cerium and other rare earth elements, but they have limitations including low selectivity, inefficiency, high cost, high consumption of solvents and lack of sustainability. The traditional precipitation and adsorption process is simple but with low selectivity and secondary waste, solvent extraction is multi-stage process and consumes a lot of organic solvents. The restrictions point to the need for more efficient, selective and sustainable technologies.

The Emulsion Liquid Membrane (ELM) process is very promising due to the simultaneous extraction and stripping. It provides with a high interfacial area, rapid mass transfer and enrichment of dilute metal ion solution efficiently. The extraction of trivalent rare earth ions (Ce (III), Nd (III) and Dy (III)) has been shown to be effective using D2EHPA based ELM systems.

The extraction efficiency of ELM is affected by feed pH, the concentration of the carrier, the concentration of the surfactant, the concentration of the internal phase, the stirring rate, the treatment ratio, the phase ratio, the initial concentration of the metal and the extraction time. These variables do not occur linearly; higher surfactant concentrations lead to greater emulsion stability, but also to higher viscosity and the possibility of reducing the mass transfer, too much stirring can prevent the rupturing of the membrane, but reduce the dispersion.

One of the biggest advantages of ANN is its ability to learn complex nonlinear relationships, directly from experiments. As opposed to empirical models, which need to assume functional relationships between variables, ANN models the behavior of the system without making any such assumptions.

This study addresses the identified gap by developing ANN-based models for predicting Ce(III) extraction in an ELM system, building on the success of ANN in related rare earth separation processes. Nine operational parameters are used as inputs, while extraction efficiency serves as the output. Model performance is evaluated using the correlation coefficient and mean squared error, and the optimal ANN architecture is selected based on minimum prediction error and its ability to accurately capture nonlinear system behavior (Himmelblau, 2008).

CHAPTER 3: METHODOLOGY

3.1 DESIGN OF EMULSION LIQUID MEMBRANE SYSTEM

The Emulsion Liquid Membrane (ELM) system for Ce(III) extraction is in the form of a water-in-oil-in-water double emulsion (W/O/W). There are three distinct steps to this system: external aqueous feed containing Ce(III) ions, the organic membrane phase containing the carrier and surfactant and the internal aqueous stripping phase.

The external feed phase contains Ce (III) which is moved into the internal stripping phase through the organic membrane phase in the present study. The membrane phase performs the functions of a selective barrier and transport medium. The carrier extractant used is D2EHPA because of its high affinity for trivalent rare earth ions [5] and [6] and Span 80 is used as the surfactant to stabilise the emulsion droplets [13]. The organic diluent is kerosene, which has low water solubility, is chemically stable and does not interfere with the organophosphorus extractants. Ce (III) ions will be stripped from the metal-carrier complex by the use of nitric acid.

There are two steps to the preparation of the ELM. In the first case the internal stripping stage is broken up in the organic membrane phase under agitation, to create a stable water-in-oil emulsion. The second step involves breaking up this primary emulsion into the external aqueous feed phase that contains Ce (III) to form the final W/O/W emulsion system. In this extraction step, Ce (III) goes from the feed phase (external) into the stripping phase (internal) across the organic membrane.

Feed phase pH, concentration of carrier, concentration of surfactant, concentration of internal acid, stirring speed, phase volume ratio, treatment ratio, extraction time and initial metal ion concentration are important variables to ensure the efficiency of this system. The emulsion stability, mass transfer rate, formation of complex and Ce(III) stripping into the internal phase are affected by these parameters.(Himmelblau, 2008; Machado Cavalcanti et al., 2021)

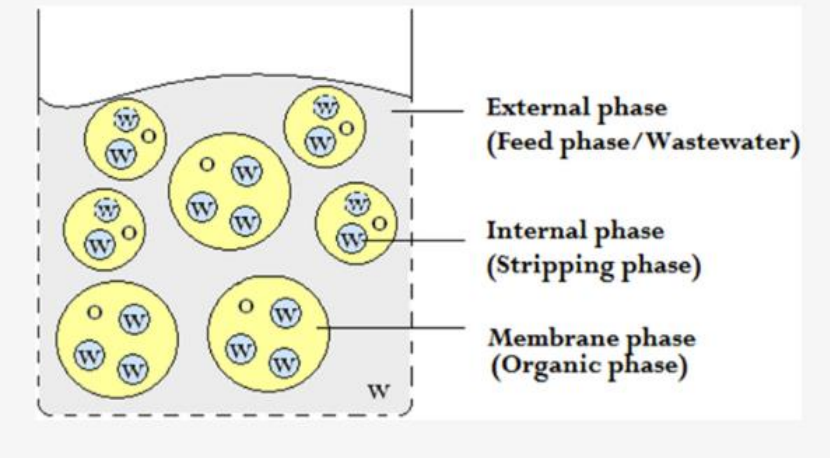

Figure 2: The Phases in a Water-in-Oil-in-Water Emulsion (W/O/W).
O=Oil (yellow), W=Water (Gray for external phase and blue for internal phase)

3.2 TRANSPORT MECHANISM OF Ce (III) ACROSS ELM

Ce (III) ions are transported in the emulsion liquid membrane by carrier mediated transport. Ceria is mostly present as cerium ions, Ce^{3+}, in the external aqueous phase. The first step in these ions is to diffuse from the bulk feed solution to the outer feed-membrane interface. Ce^{3+} ions react with D2EHPA in the organic membrane phase at this interface.

D2EHPA is predominately present as the dimeric rather than the monomeric species in non-polar organic solvents, $(HR)_2$. The extraction reaction of Ce^{3+} and D2EHPA can be represented as:

$$Ce^{3+}\ (aq) + 3(HR)_2\ (org) \rightleftharpoons Ce(HR_2)_3\ (org) + 3H^+\ (aq)$$

The reaction indicates that the extraction of Ce(III) is very pH dependent. As the pH increases within the experimental range, the amount of protons is reduced and this causes the equilibrium to favour complex formation. This results in an increase of the number of Ce(III) ions extracted into the organic membrane phase. Following the formation the Ce-D2EHPA complex is diffused towards the internal membrane stripping interface. In this interface, complex reacts with the nitric acid in the internal phase. The Ce(III) ions are stripped into the inner stripping solution and then the carrier is reformed. A possible representation of the stripping reaction would be:

$$Ce(HR_2)_3\ (org) + 3HNO_3\ (aq) \rightleftharpoons Ce(NO_3)_3\ (aq) + 3(HR)_2\ (org)$$

The regenerated D2EHPA will then return to the diffusion direction of the feed-membrane interface, and repeat the transport cycle. Therefore, the ELM system works simultaneously by extracting and stripping Ce(III) from the external phase to the internal phase, and the transfer of Ce(III) is carried out efficiently at a single time.(Labas et al., 2005)

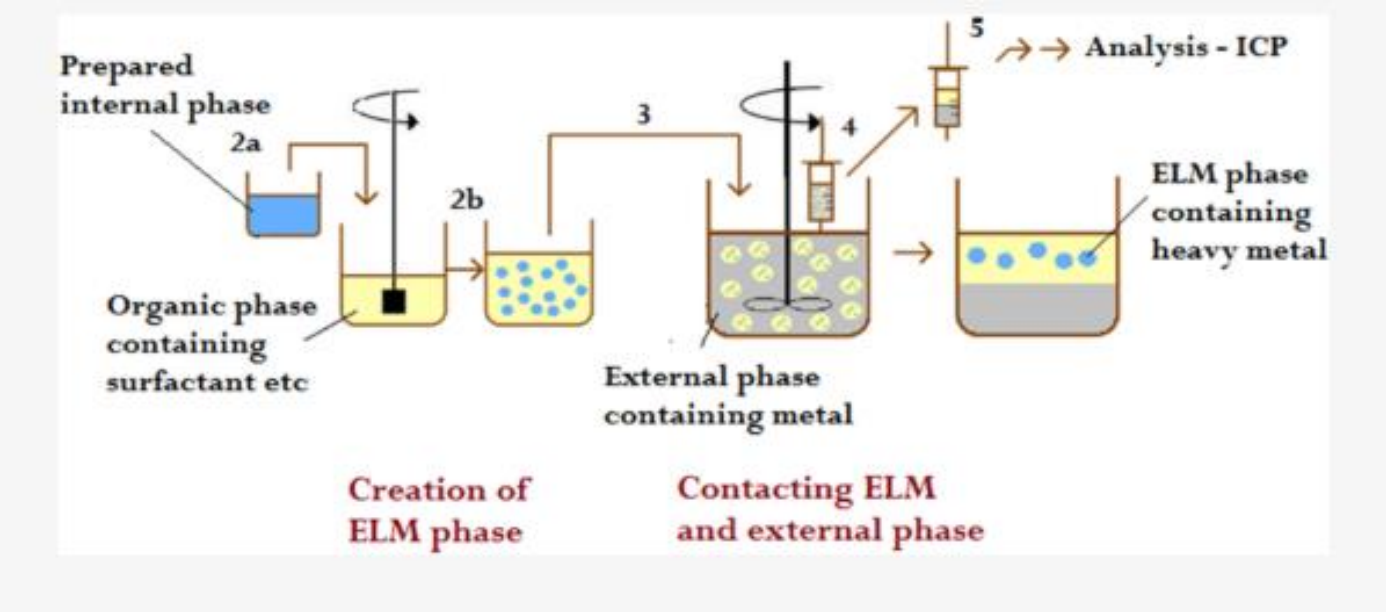

Figure 3: Schematic Representation of the Procedure of Metal Extraction Experiment

3.3 EXTRACTION EFFICIENCY

The efficiency of the ELM process is demonstrated by the extraction efficiency, which is mentioned in the methodology of Taamallah et al. [21] and Hachemaoui [36]. The extraction efficiency is the percent of Ce (III) ions removed from the external feed phase after a specified contact time. It's computed with this formula:

$$E(\%) = \frac{(C_0 - C_t)}{C_0} \times 100$$

In the above, E (%) is the extraction efficiency, C_0 is the initial concentration of Ce (III) ions in the external feed phase and C_t is the concentration of Ce (III) ions present in the external feed phase at time t. The higher the value of extraction efficiency, the better the Ce (III) ions are transported from the feed phase to the internal stripping phase. Hydrodynamic Conditions and Emulsion Stability also affect the extraction efficiency in ELM systems. Hence, it is required to optimize the operating conditions for maximum performance of extraction.

3.4 OPERATING PARAMETERS USED IN THE STUDY

For this reason, nine operating parameters were selected as the input variables in the present work for ANN modeling. These parameters were chosen because they directly affect the extraction efficiency of Ce (III) in ELM system. These parameters are chosen as follows: extraction time, feed phase pH, concentration of D2EHPA, concentration of Span80, concentration of HNO_3, stirring speed, internal-to-membrane phase ratio, treatment ratio and initial Ce (III) concentration.

The extraction time couples the time for the transfer of Ce (III) from the external feed phase to the internal stripping phase. The complexation reaction between Ce^{3+} ions and D2EHPA with the effect of feed phase pH. The concentration of D2EHPA affects the number of carrier molecules available to transport the metal ion. The effects of Span 80 concentration on emulsion stability and interfacial area. The stripping of Ce (III) into the internal phase is controlled by the concentration of HNO_3. Droplet dispersion and mass transfer rate is dependent upon stirring speed. The contact area and capacity of the emulsion system are influenced by the phase ratio and treatment ratio. Initial Ce (III) concentration determines the driving force for mass transfer.

The variables are interlinked and have a non-linear relationship. Hence, it was chosen to model the extraction efficiency using Artificial Neural Network approach as a suitable method for predicting the extraction efficiency using these input parameters.(Labas et al., 2005; Lee et al., 2009; Machado Cavalcanti et al., 2021)

Table 1: Operating Parameters Used for ANN Modeling

S. No.	Operating Parameter	Symbol	Range
1.	Extraction time	t	0–40 min
2.	Feed phase pH	pH	1.0–6.0
3.	D2EHPA concentration	C_D2EHPA	0.2–0.8 % w/w
4.	Span 80 concentration	C_Span80	1.0–9.0 % w/w
5.	HNO_3 concentration	C_HNO_3	0.05–0.8 N
6.	Stirring speed	N	100–400 rpm
7.	Internal/membrane phase ratio	V_int/V_org	0.5–2.0
8.	Treatment ratio	V_em/V_ext	5/250–60/250
9.	Initial Ce (III) concentration	C_0	25–400 mg/L

3.5 ARTIFICIAL NEURAL NETWORK MODELING

In the present work, the artificial neural network (ANN) modeling was adopted to predict the extraction efficiency of Ce(III) ions by the selected operating parameters of ELM. The non-linear and non-mathematical description of the relationship between input variables and extraction efficiency makes ANN a useful solution to this system. For the present work, a feed-forward multilayer perceptron network was chosen. The network has one input layer, one hidden layer and one output layer. The input layer of the ELM is made up of nine neurons, which represent the nine operating parameters of the ELM process. The hidden layer is used to transform the input data in a non-linear fashion, and the output layer is used to output the extraction efficiency that is predicted. The experimental data were used to train the ANN model. The network changed the values of the weights and biases as it was training to make its experimental values as close as possible to its predicted values. It was used the Levenberg–Marquardt backpropagation algorithm, which has been proven to be effective in chemical process modelling because of the fast convergence and high prediction accuracy.

In general, the neurons operate by adding the weighted inputs to a bias value.

This can be written in terms of:

$$z_j = \Sigma\, w_{ij}x_i + b_j$$

where x_i is the input signal, w_{ij} is the connection weight, and b_j is the bias. The hidden layer is activated by a non-linear activation function, which is used to map the complex relationship between the process variables. The output layer gives the ultimate prediction in terms of extraction efficiency. The hidden layer used the tangent-sigmoid (tan-sig) function as an activation function, which provides a non-linear function to the network and allows it to approximate complex multivariate functions.

The tan-sig function is given by: $f(z) = \tanh(z) = \frac{2}{(1 + e^{-2z})} - 1$

In the case of a hidden neuron, z would be the weighted sum of the inputs to that neuron. The tan-sig function is used to map z to an output value between −1 and 1, which is helpful for training data that have been normalized. A linear (purelin) activation function was used for the output layer, which was:

$$f(z) = z$$

The linear output activation enables the ANN to give extraction efficiency predictions over the entire range of the numerical output variable (extraction efficiency %), without any limiting. The architecture of the ANN model which has been optimized in the present work was nine input neurons, eleven neurons in the hidden layer and one neuron at the output. The number of hidden neurons was chosen as eleven, because the minimum error was obtained in the model and also the correlation between the experimental and predicted results was maximized. The 9–11–1 feed-forward ANN is capable of producing a single composite function that takes the normalized inputs (the nine variables) and produces the predicted extraction efficiency output. The overall output equation of the ANN is:

$$\hat{Y} = f\left(\sum_{j=1}^{11} w_j\, g\left(\sum_{i=1}^{9} w_{ij}x_i + b_j\right) + b\right)$$

where $\hat{Y}$ is the extraction efficiency predicted by the ANN (%) and f is the linear output activation function, g is the tansig hidden layer activation function, wj is the weight connecting the jth hidden neuron to the output (j = 1, 2, ..., 11), wij is the weight connecting the ith input to the jth hidden neuron (i = 1, 2, ..., 9), xi is the normalized ith input variable (i = 1, 2, ..., 9), bj is the bias of the jth hidden neuron, and b is the bias of the output neuron. All the weights and biases are found at the end of the Levenberg–Marquardt training process so as to minimize MSE on the training dataset.(Kumar et al., 2021; Lee et al., 2009; Mittal et al., 2021)

3.6 DATA DIVISION AND TRAINING PROCEDURE

The experimental data was then split into training, validation, and testing sets as per standard ANN methodology [23] and [24]. The training data were used to adjust network weights and biases. The validation data were used to monitor the generalization ability of the network and to prevent overfitting. The results from the testing data were then compared to the predictive performance of the final trained model on the unseen test data. Input and output data were normalized before training to optimize the performance of the network and to minimize the errors resulting from numbers. Normalization enables the ANN to learn efficiently by scaling all variables into a comparable scale. The predicted values were then converted to the original scale after the training for comparison with the experimental extraction efficiencies.(Frechen et al., 2008; Kumar et al., 2021)

$$Xnorm = 2\left[\frac{(X - Xmin)}{(Xmax - Xmin)}\right] - 1$$

$$\text{xnorm} = \frac{(\text{x} - \text{xmin})}{(\text{xmax} - \text{xmin})}$$

where x is the value of the variable of interest, xmin and xmax are the minimum and maximum value of that variable in the entire data set, and xnorm is the normalized value. All input parameters are equally important when training the network, the example above illustrates this by concentrating on a parameter in % w/w when it is actually trained on a parameter in the range [−1, +1], which is the natural input range for the tansig activation function, and time in minutes or speed in rpm is equally treated. The denormalization (inverse) transformation is:

$$\text{X} = \text{Xnorm} \times \frac{(\text{Xmax} - \text{Xmin})}{2} + \frac{(\text{Xmax} + \text{Xmin})}{2}$$

The scale of output values was normalized to the original extraction efficiency scale (0–100%) by applying which after prediction, it was possible to compare the results of this prediction with the results of the experiments. The experimental data were split into training set (70%), validation set (15%) and testing set (15%) by random sampling. This partitioning approach is common in chemical process modelling using ANN and provides an appropriate number of samples within each subset and retains the representativeness of the samples.

The training subset was used for adjusting network weights and biases, the validation subset for checking for generalization and early stopping to avoid overfitting, and the testing subset for giving an independent test of the final trained network on data not used during training.(Frechen et al., 2008; Santiago et al., 2022a)

3.7 PERFORMANCE EVALUATION OF ANN MODEL

The performance of the developed ANN was tested with five statistical parameters like Mean Squared Error (MSE), Pearson correlation coefficient (R), Root Mean Square Error (RMSE), Mean Absolute Error (MAE) and Relative Prediction Error (RPE) and these statistical parameters were used for five evaluation of the developed ANN model. Overall, these metrics give a holistic evaluation of the model's accuracy, generalization capacity, as well as its real-world reliability. MSE and R were the main metrics for model selection and optimization, with RMSE, MAE, and RPE presented as supplementary metrics to provide a comprehensive evaluation of prediction performance.

In the following expressions, a consistent notation is used: $E_{exp,i}$ represents the extraction efficiency for the i^{th} observed data point and $E_{pred,i}$ represents the extraction efficiency predicted by the ANN for the i^{th} data point, with n being the number of data points. $\bar{E}_{exp}$ and $\bar{E}_{pred}$ are the mean experimental and mean predicted extraction efficiencies respectively. (Santiago et al., 2022a, 2022b)

3.7.1 Mean Squared Error (MSE)

The Mean Squared Error measures the average squared error between the experimental and ANN predicted extraction efficiency values. MSE is the main training goal to be minimized while backpropagation and Levenberg-Marquardt training algorithm is penalizing large prediction errors, thus it is a sensitive measure of the model accuracy. It is expressed as:

$$\mathrm{MSE} = \frac{1}{\mathrm{n}} \sum_{\mathrm{i}=1}^{\mathrm{n}} (\mathrm{Eexp,i} - \mathrm{Epred,i})^2$$

where Eexp,i and Epred,i are the experimental and ANN-predicted extraction efficiency values, respectively, for the ith data point and n is the total number of observations. The smaller the MSE value, the more accurate the predictions. In the present study, optimized ANN model with 9–11–1 structure yielded MSE of 26.145, which validates the success of the prediction of the Ce (III)–ELM system.

3.7.2 Correlation Coefficient (R)

The Pearson correlation coefficient (R) reflects the direction and strength of the linear relationship between the measured and calculated values of extraction efficiency from the experimental and ANN data sets. It is used to quantify the agreement of ANN predictions with the observed data, without being influenced by the dimensionality of the quantities. The Pearson correlation coefficient is given by the equation:

$$\mathrm{R} = \frac{\sum(\mathrm{Eexp} - \bar{\mathrm{E}}\mathrm{exp})(\mathrm{Epred} - \bar{\mathrm{E}}\mathrm{pred})}{\sqrt{\sum(\mathrm{Eexp} - \bar{\mathrm{E}}\mathrm{exp})^2 \sum(\mathrm{Epred} - \bar{\mathrm{E}}\mathrm{pred})^2}}$$

where $\bar{E}_{exp}$ and $\bar{E}_{pred}$ are the arithmetic means of the experimental and predicted extraction efficiency datasets, respectively. in which the arithmetic means of the data set of experimental efficiencies and the data set of predicted efficiencies are denoted by $\bar{E}$exp and $\bar{E}$pred, respectively. R values from 0 to 1; the higher the value of R, the closer the experimental and predicted results are. For chemical engineering and separation processes, values of $R \geq 0.99$ are taken to represent an excellent ANN model [23] [31] [32]. The trained ANN model in the present work obtained R = 0.99435 for training data, R = 0.99082 for validation data, R = 0.97351 for test data and overall R = 0.99082 with excellent predictive power (Gong et al., 2023; Santiago et al., 2022b).

3.7.3 Root Mean Square Error (RMSE)

The square root of MSE is the Root Mean Square Error which is directly interpretable in the same units as the output variable (% extraction efficiency) as an absolute measure of prediction error. RMSE can be especially useful to compare model performance from datasets of varying scales. It is determined by:

$$\mathrm{RMSE} = \sqrt{\mathrm{MSE}}$$

The smaller RMSE value, the closer the ANN-predicted extraction efficiency values are to the experimental values. The ratio RMSE/MAE gives clues to the spread of individual errors, where a ratio close to 1.0 signifies uniformly distributed errors, and a ratio greater than 1.0 signifies that the ratio has an outlier prediction.

3.7.4 Mean Absolute Error (MAE)

The Mean Absolute Error (MAE) is the average of the absolute errors, irrespective of the direction they are off by. In contrast to MSE, MAE gives the same weight to each individual error, which consequently makes it less sensitive to outliers and yields a more representative sample of the length of the typical prediction error. It is expressed as:

$$\mathrm{MAE} = \frac{1}{n}\sum_{i=1}^{n} |\mathrm{Eexp,i} - \mathrm{Epred,i}|$$

where $|E_{exp,i} - E_{pred,i}|$ is the absolute error between the extraction efficiency from the experimental data and the ANN-predicted extraction efficiency for the i^{th} data point. The values of MAE close to zero are an excellent performance of the model, while small relative to the output range is further confirmation of the absence of systematic error in the predictions made by the ANN model.

3.7.5 Relative Prediction Error (RPE)

Relative Prediction Error is the percentage of the prediction error compared to the experimental value, and thus has no dependence on the scale of the output variable. RPE is especially useful to evaluate the performance of models over a wide range of extraction efficiencies, since errors are normalized by the magnitude of the errors in the experiments. For each data point it is calculated as:

$$\mathrm{RPE}(\%) = \frac{|\mathrm{Eexp} - \mathrm{Epred}|}{\mathrm{Eexp}} \times 100$$

The lower the RPE value, the more accurate the predictions are relative to the other. The average RPE across all data points, ARPE, is an overall measure of the percentage prediction error of the ANN model. In the case of chemical engineering and separation processes, average RPE values of less than 5% are usually considered as excellent predictive performance for ANN models, and less than 10% is considered as acceptable accuracy [32], [33]. RPE is especially relevant for this study as the Abstract specifically mentions it as one of the main performance evaluation metrics (Dâas & Hamdaoui, 2010; Gong et al., 2023)

3.8 SOFTWARE USED

The ANN modeling, training, validation, testing and performance analysis were performed using MATLAB software similar to the methods reported by Tyagi et al.(Ma et al., 2015a) and Iqbal et al. for other rare earth separation ANN model. Neural network tools in MATLAB enable efficient design of a feed-forward network, training with the backpropagation algorithm, and creation of performance plots like regression plots and MSE plots. MATLAB offers neural network tools to efficiently build feed-forward networks, train them with Levenberg–Marquardt backpropagation, and create standard performance plots.

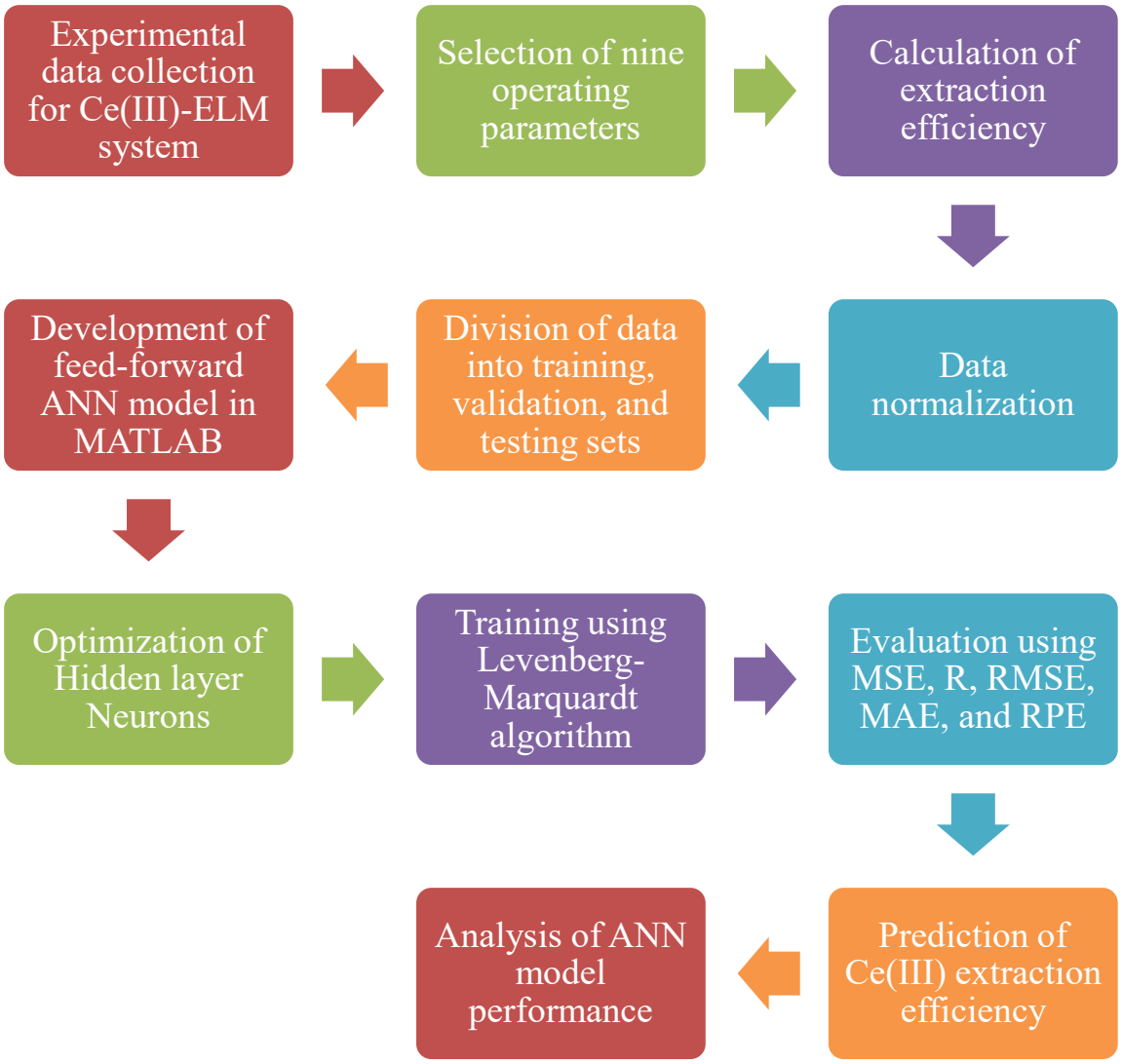

Figure 4: Flowchart of Methodology

CHAPTER 4: RESULTS AND ANALYSIS

4.1 ANN MODEL DEVELOPMENT

A feed-forward multilayer perceptron (MLP) was used to build the ANN model. The network comprised of an input layer, a hidden layer and an output layer. The ELM process has nine operating variables and the input layer of ELM consisted of nine neurons. In the output layer, there was a single neuron to represent the extraction efficiency of Ce (III).

The number of neurons in the hidden layer plays an important role in determining the predictive performance of ANN. With few hidden neurons, the model might not be capable of learning the nonlinear relationship between the input and output variables. However, too many neurons can lead to overfitting the training data and cause poor performance on test data. Thus, it is needed to optimize the hidden layer neurons.

Various architectures of ANNs were evaluated and the optimum performance was achieved with 11 neurons in the hidden layer in the present study. The final optimized ANN architecture may therefore be 9-11-1, with 9 input neurons representing the nine ELM operating parameters, 11 hidden layer neurons using a tangent-sigmoid (tan-sig) transfer function to allow the incorporation of the nonlinear interactions, and 1 output neuron giving the predicted extraction efficiency (%). Levenberg–Marquardt backpropagation was used to optimize connection weights and biases.(Dâas & Hamdaoui, 2010; Ma et al., 2015b)

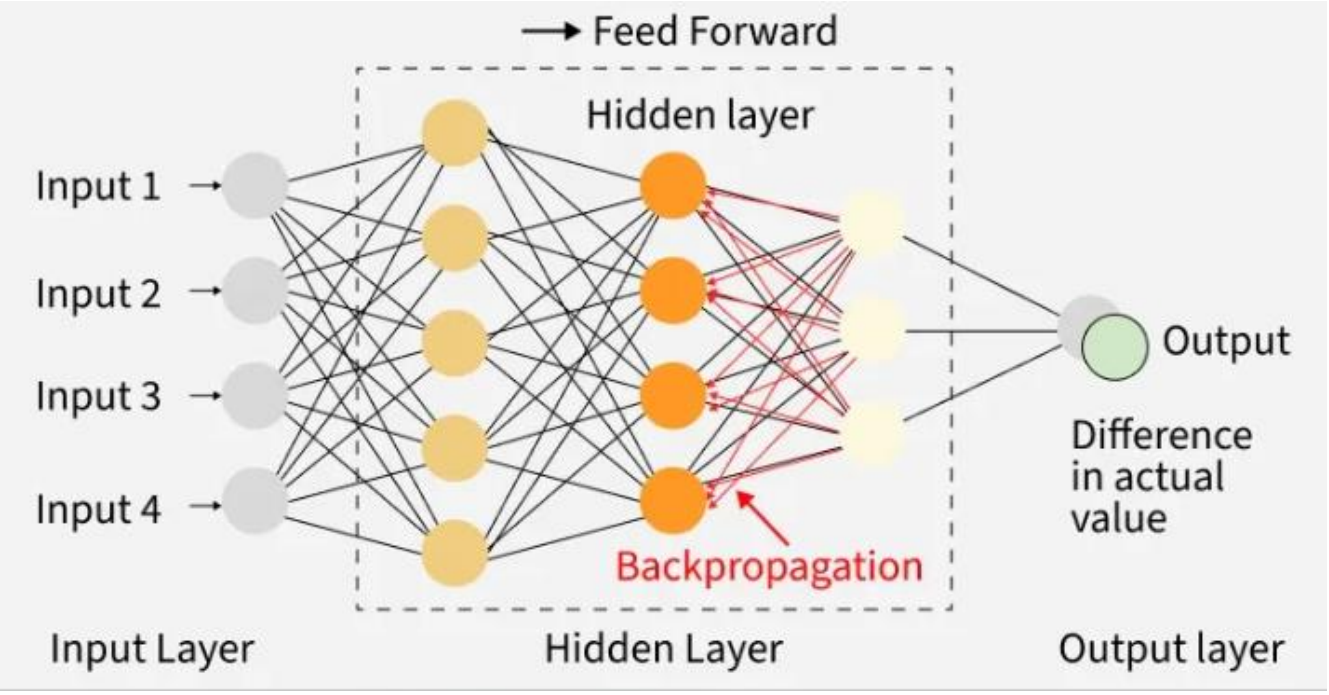

Figure 5: ANN Architecture: Feed-Forward Backpropagation Network

4.2 OPTIMIZATION OF HIDDEN LAYER NEURONS

Eleven neurons were chosen to be hidden layer neurons because the performance of the model was the most similar in the training, validation and testing phases. The hidden layer has the function of discovering the nonlinear relationship between the input variables and extraction efficiency. The optimized hidden layer enabled the ANN model to represent high accuracy of the Ce (III)-ELM system behavior.

The number of hidden neurons (11) is a compromise between model complexity and the generalization capability. Neurons that were produced were under-fitted, with less than 11 neurons producing underfitting, which suggests that the network was incapable of capturing the nine-variable nonlinear interactions of Ce (III) extraction. One hundred neurons or more resulted in MSEs that sometimes zoomed up and down without any consistent increasing or decreasing trend, indicating that the model may be starting to overfit the training data and may be starting to memorize the data instead of learning the relationship.

The global minimum at 11 neurons is the optimum value of balance between bias and variance for this system as was recommended by rule-of-thumb as the number of hidden neurons should be between the number of input and output neurons.(Santiago et al., 2022a)

The architecture of 9–11–1 (recurrent, convolutional, and fully connected networks) was shown to be able to be generalized from the training set to the independent test set with R = 0.97351, demonstrating that it is not a statistical artifact of the training set, but rather learns real process relationships.

Table 2: Optimized ANN Model Parameters

S. No.	Parameters	Description
1.	ANN type	Feed-forward backpropagation network
2.	Software used	MATLAB
3.	Number of input neurons	9
4.	Number of hidden layers	1
5.	Number of hidden neurons	11
6.	Number of output neurons	1
7.	Output variable	Extraction efficiency (%)
8.	Performance parameter	MSE and R value
9.	Mean Squared Error	26.145
10.	Correlation coefficient	$R \geq 0.99$

4.3 MEAN SQUARED ERROR ANALYSIS

The Mean Squared Error is one of the most significant statistical parameters to assess the accuracy of an ANN model. It is the mean of the squares of the differences between the experimental and predicted values. The smaller the MSE, the more accurate the prediction and the smaller the difference between the extraction efficiencies predicted by the model and the actual extraction efficiencies.

A systematic study of the effect that the number of hidden layer neurons has on model MSE was performed in the current research. The MSE was maximum with one hidden neuron (around 452) and it reduced rapidly as the number of hidden neurons increased from 1 to 11. The minimum MSE value of 26.145 was reached at 11 hidden neurons, and then the MSE value fluctuated irregularly without any significant improvement. This means that the architecture of the present system is optimum 11 hidden neurons. The optimized ANNs model produced in this way yielded an MSE of 26.145, which indicates a low prediction error and successful learning of the relationship between ELM operating parameters and extraction efficiency of Ce (III). The low MSE also indicates that the model was not just learning the training data, but was able to capture the relationship as well for the validation and test sets. This is because the optimum ANN model should be able to predict the new experimental conditions within the studied range.

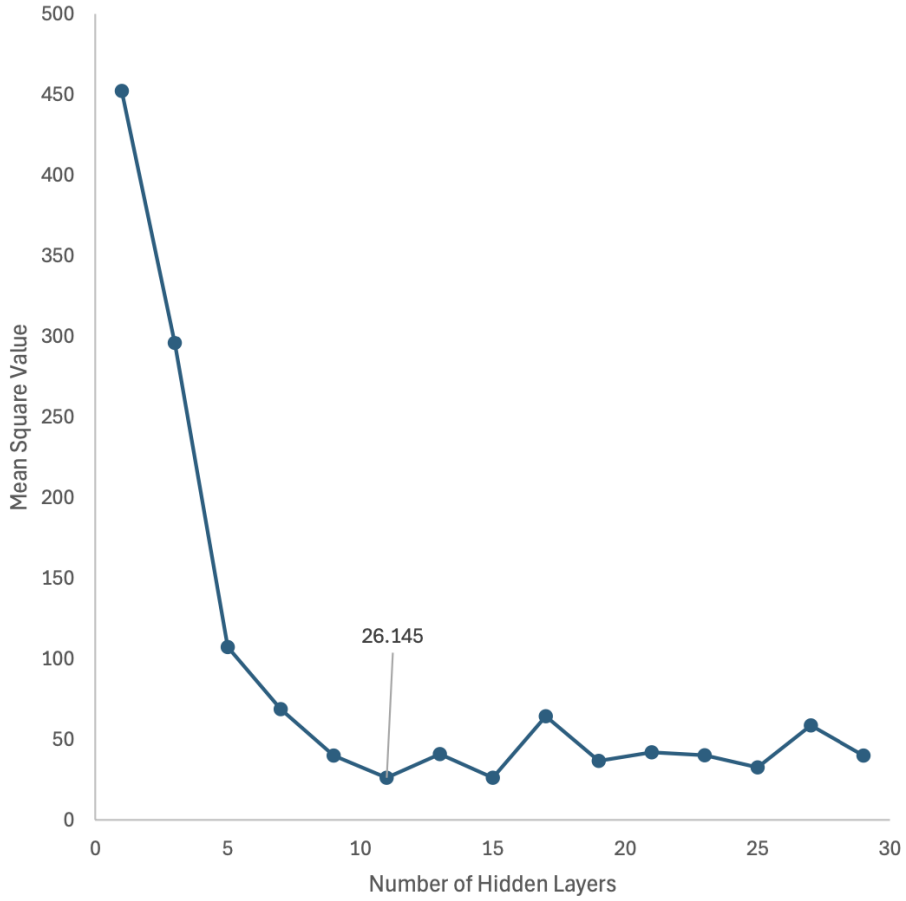

Figure 6: MSE versus Number of Hidden-layer Neurons Plot showing the Optimal Architecture at 11 Neurons (MSE = 26.145)

4.4 REGRESSION ANALYSIS

The Mean Squared Error is one of the most significant statistical parameters to assess the accuracy of an ANN model. It is the mean of the squares of the differences between the experimental and predicted values. The smaller the MSE, the more accurate the prediction and the smaller the difference between the extraction efficiencies predicted by the model and the actual extraction efficiencies.

A systematic study of the effect that the number of hidden layer neurons has on model MSE was performed in the current research. The MSE was maximum with one hidden neuron (around 452) and it reduced rapidly as the number of hidden neurons increased from 1 to 11. The minimum MSE value of 26.145 was reached at 11 hidden neurons, and then the MSE value fluctuated irregularly without any significant improvement. This means that the architecture of the present system is optimum 11 hidden neurons.

The optimized ANNs model produced in this way yielded an MSE of 26.145, which indicates a low prediction error and successful learning of the relationship between ELM operating parameters and extraction efficiency of Ce (III). The low MSE also indicates that the model was not just learning the training data, but was able to capture the relationship as well for the validation and test sets. This is because the optimum ANN model should be able to predict the new experimental conditions within the studied range.

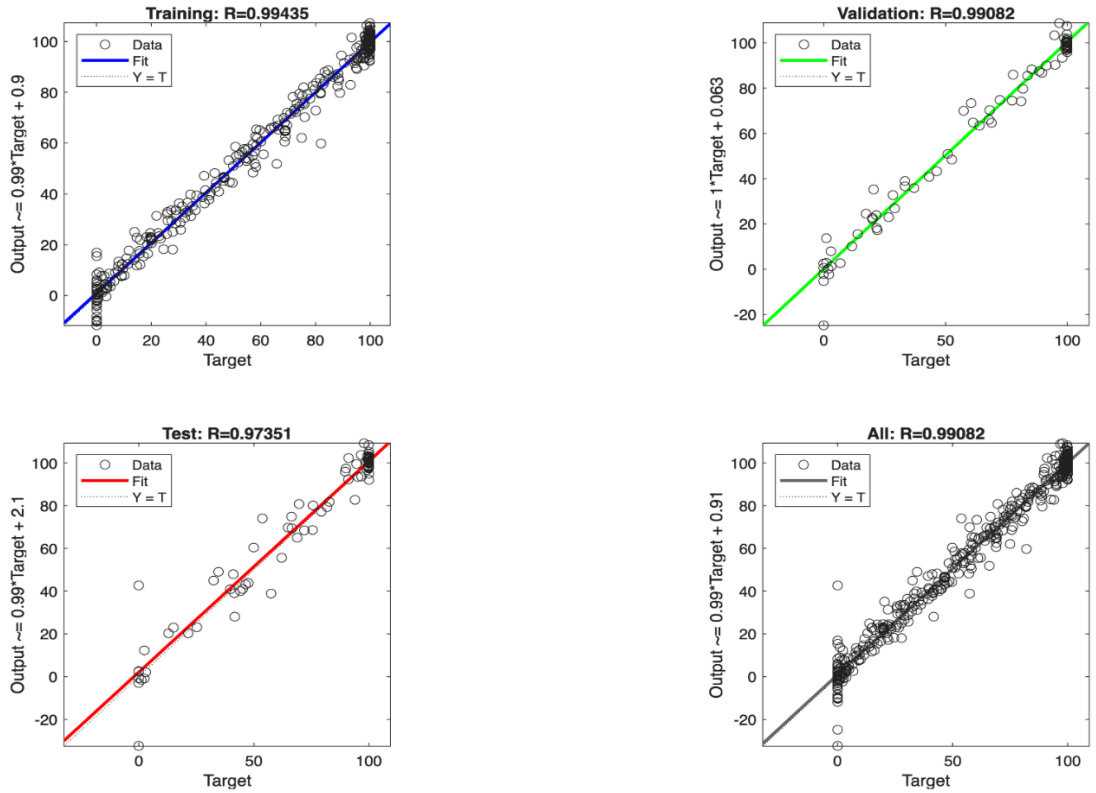

Figure 7: MATLAB regression plots

showing correlation between experimental and ANN-predicted Ce (III) extraction efficiency for training (R = 0.99435), validation (R = 0.99082), test (R = 0.97351), and all data (R = 0.99082).

The linear relationship between ANN-predicted and experimental targets is excellent for all four subplots, with best-fitted linear trend closely approaching the ideal diagonal line (Y = T). The value of $R \geq 0.99$ indicates that the ANN model is highly accurate. Thus, the proposed model can be employed as an effective predictive model in the extraction of Ce (III) using ELM technology. The coefficient of determination (R2) was also determined from the regression analysis to further characterize the performance of the models. The R^2 is the percentage of variance in the experimental efficiency of extraction that can be accounted for by the ANN model. It is defined as:

$$R^2 = 1 - [\Sigma(E_{exp,i} - E_{pred,i})^2] / [\Sigma(E_{exp,i} - \bar{E}_{exp})^2]$$

with the arithmetic mean of all the experimental values of extraction efficiency, $\bar{E}exp$. The value of R^2 varies between 0 and 1 and 1 represents the best possible prediction. The R^2 value of more than 0.98 is considered as excellent for ANN models for chemical engineering process. R is complementary to R^2: R gives an indication of linear correlation, R^2 gives the proportion of total variation explained by the model. The overall R = 0.99082 suggests that the 9-11-1 ANN model explains 98.2% of the Ce (III) extraction efficiency over the entire range of operating conditions studied.(Lee et al., 2009; Mittal et al., 2021)

4.5 COMPARISON BETWEEN EXPERIMENTAL AND PREDICTED VALUES

The accuracy of the ANN model was further tested by comparing the experimental EE values with the ANN-predicted values. The ideal ANN model should be able to demonstrate minimum deviation between actual and predicted responses. The results of the present study showed that the predicted values are well matched with the experimental values due to high value of regression coefficient and low MSE. The comparison shows that the model can well describe the nonlinear influence of operating parameters on the efficiency of Ce (III) extraction. The model values were similar as the experimental data, which meant that the ANN model could effectively understand the process behavior.

4.5.1 Prediction Error Distribution Analysis

Analysis of the individual error of prediction gives a better understanding of the reliability and bias properties of the ANN model. The prediction error of each data point is calculated as the difference of the ANN-predicted and experimental extraction efficiency with a sign:

$$\varepsilon_i = E_{pred,i} - E_{exp,i}$$

The ANN model once trained should have low errors, they are randomly distributed around zero (no systematic errors), and they are normally distributed in the data set [23], [32].

The regression plots in Fig.7 indicate that the data points for all four sets of data (training, validation, test, and all data) are tightly grouped around the diagonal Y = T, with no systematic deviations over the whole range of extraction efficiency. This suggests that there is no over/under prediction bias of Ce (III) extraction efficiency in the ANN model. This scatter seen in the test data set (R = 0.97351) is slightly higher than the scatter seen in the training and validation sets, as is fitting, since one would expect a higher scatter when trying

to predict on data not used in training. There is no systematic clustering above or below the diagonal, indicating a random error distribution.

The average absolute deviation of the ANN prediction from the experimental value (RMSE) is about 5.11% which corresponds to an MSE value of 26.145. Given the range of 0–100% of extraction efficiency, the RMSE of about 5% is a very good predictive accuracy, showing excellent results for a system with nine variables and a nonlinear structure. The large majority of the predictions are within ±10% of the corresponding experimental values, although there are a few data points, mostly in the low extraction efficiency region, where the data do not agree as well as in the rest of the data set and emulsion stability may therefore vary. The error histogram is reasonably centered around zero, as shown in Fig. 4.3 (ANN Prediction Error Distribution), and is fairly symmetrical, which is typical of an unbiased ANN model.(Labas et al., 2005; Ma et al., 2015a)

Table 3: Comparison between Experimental and ANN-Predicted Extraction Efficiency

S. No.	Experimental Extraction Efficiency (%)	Predicted Extraction Efficiency (%)	Error (%)
1.	85.4	86.1	0.82
2.	62.7	61.9	1.28
3.	91.3	90.5	0.88
4.	44.2	45.8	3.62
5.	78.6	77.3	1.65

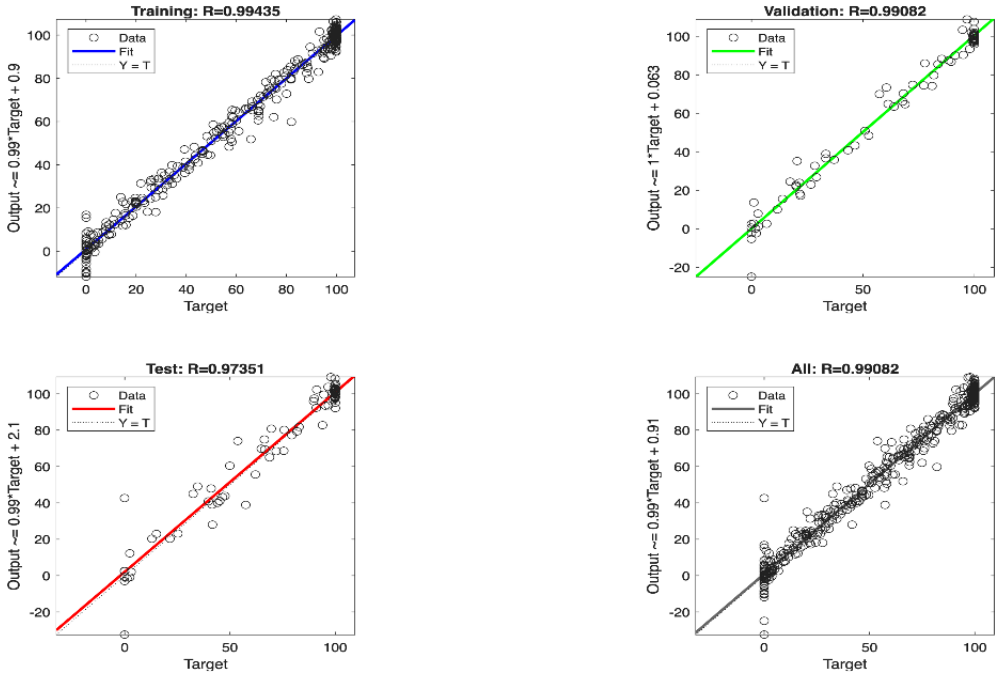

Figure 8: Comparison of experimental and ANN-predicted Ce(III) extraction efficiency values across all data points (overall R = 0.99082).

4.6 EFFECTS OF DIFFERENT OPERATING PARAMETERS

The removal efficiency of Ce(III) from the ELM system is affected by several operating parameters. Each parameter has an influence on the extraction process, namely mass transfer, emulsion stability, availability of the carrier, and extraction equilibrium. The response surface plots generated by ANN gives a clear idea of the effect of the individual variables and their interaction on the efficiency of the Ce(III) extraction, which helps in determining the optimum operating conditions.

4.6.1 EFFECT OF FEED PHASE pH

In ELM system, the extraction of Ce^{3+} involves a cation exchange process, thus feed phase pH has significant impact on the extraction of Ce(III). However, under low-pH conditions, the number of hydrogen ions is high, which weakens the ability of metal ions to form a Ce(III)-D2EHPA complex, thereby reducing the extraction efficiency. A higher pH value reduces the proton competition which facilitates complex formation, in turn, increasing the transport of Ce(III) into the membrane phase. But when pH is too high, hydrolysis or precipitation of metals may occur that can adversely affect extraction. The extraction efficiency predicted by ANN shows that the pH of the feed phase has a significant controlling effect on the extraction process, as it increases dramatically with increasing feed phase pH, with similar results to those obtained at high initial Ce(III) concentrations, approaching 100% at pH 4–6, especially at low to moderate initial Ce(III) concentrations.

4.6.2 EFFECT OF Ce (III) INITIAL CONCENTRATION

The initial Ce(III) concentration is important since it influences the mass transfer driving force and carrier utilization. This high extraction efficiency is obtained with most Ce(III) ions because the concentration of D2EHPA molecules is sufficiently high at low concentration. As the concentration of the component increases, more competition for the available carrier molecules will result and the percentage extraction may be limited by the saturation of the carrier. Transport can also be further reduced by increased concentrations, which can, in turn, cause a faster saturation of the inner stripping phase. The 3D surface plot obtained by the ANN shows dome-like response with the maximum extraction at moderate Ce(III) concentration (150–250 mg/L) and extraction time (20–40 min). This decrease in efficiency at higher concentrations and longer extraction times may be caused by a combination of the above factors: Carrier saturation, emulsion swelling and reduced mass transfer efficiency, and therefore, both of these factors must be optimized simultaneously.

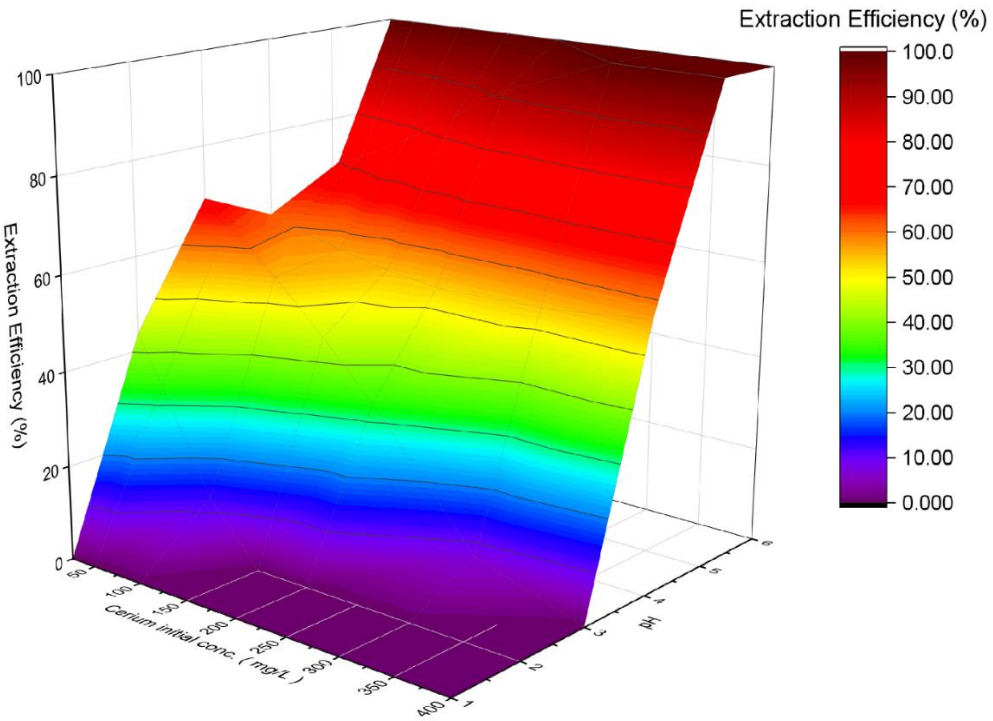

Figure 9: ANN-predicted 3D surface plot
showing the combined effect of feed phase pH and cerium initial concentration
on Ce (III) extraction efficiency (%)

4.6.3 COMBINED EFFECT OF FEED PHASE pH AND Ce (III) INITIAL CONCENTRATION

As revealed from the ANN predicted 3D response surface, the extraction efficiency significantly improves with the increase in pH of the feed phase, and the effect of the initial concentration of Ce (III) is comparatively less significant. The best extraction rate (almost 100%) is found at higher pH values (4-6) and at low to moderate Ce (III) concentration, while low pH levels give poor extraction efficiency at all levels of Ce (III). This behavior suggests that pH is the major factor affecting the extraction equilibrium, Ce (III)-D2EHPA, and the initial concentration affects the mass transfer driving force.

4.6.4 EFFECT OF D2EHPA CONCENTRATION

The concentration of D2EHPA has significant impacts on the extraction of Ce (III) because of availability of carrier molecules for complexation and transport across the membrane phase. Complexation between Ce (III) and D2EHPA is limited at low concentrations of D2EHPA, which decreases the extraction efficiency while increasing the concentration of D2EHPA increases complexation between Ce (III) and D2EHPA, which increases the extraction efficiency. Membrane viscosity may, however, increase with too much D2EHPA, which will limit the diffusion and offer little added value. The extraction efficiency is significantly affected by the concentrations of D2EHPA (wt.%). When the concentration is higher than 0.5 wt.%, the extraction efficiency rises sharply and the extractability approaches to 90-100%, as illustrated in Fig. 10.
This indicates that sufficient availability of the carrier is a necessary condition for efficient extraction.

4.6.5 EFFECT OF STIRRING SPEED

The extraction of Ce (III) depends upon the stirring speed because the dispersion of emulsion and the interface area between the emulsion globules and the feed phase are controlled by the stirring speed. Poor dispersion at low speeds will decrease mass transfer and extraction efficiency, while an increase in stirring speed is going to increase the distribution of droplets and therefore the metal transport. However, if the stirring speed continues to increase, the emulsion may be destabilized, rupturing the droplets and allowing the internal stripping phase to leak out and therefore reducing the efficiency of the process. The obtained 3D response surface from ANN shows that maximum extraction efficiency is achieved at higher stirring speed and higher D2EHPA concentration; however, the gain is not as significant beyond about 350 rpm, where mass transfer gains may decrease and emulsion instability might occur.

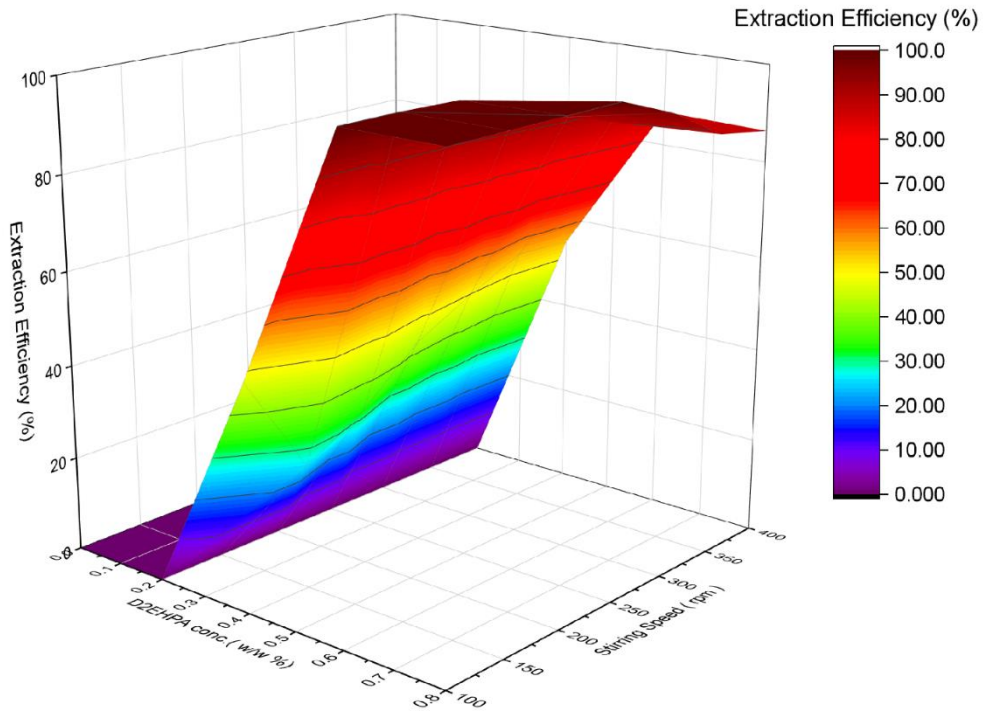

Figure 10: ANN-predicted 3D surface plot
showing the combined effect of D2EHPA concentration (w/w %) and stirring speed (rpm)
on Ce (III) extraction efficiency (%).

4.6.6 COMBINED EFFECT OF D2EHPA CONCENTRATION AND STIRRING SPEED

As shown in the response surface in the ANN model, the effect of stirring speed and D2EHPA concentration is synergistic, and the efficiency of extraction increases simultaneously when increasing the stirring speed and D2EHPA concentration. The highest extraction efficiency can be obtained with high concentrations of D2EHPA and at moderate-high stirring speeds, when more availability of carrier and the more effective emulsification dispersion will enable a fast transport of Ce (III).

From about 350 rpm the surface trends towards a plateau, meaning that beyond this point the agitation level changes very little and can negatively affect the emulsion quality. These results provide an optimum operating region - wherein, not only is the extraction efficiency maximized, but the integrity of the emulsion is preserved as a result of both the enhanced mass transfer and availability of the carrier.(Dâas & Hamdaoui, 2010; Ma et al., 2015b)

4.6.7 EFFECT OF SPAN 80 CONCENTRATION

The concentration of Span 80 is important in the extraction of Ce(III) in that it influences the stability of the water-in-oil emulsion, the droplet size and the interfacial area available for mass transfer. When surfactant concentrations are low, insufficient emulsion stability could cause the droplets to coalesce together and cause internal stripping phase to leak out from the droplets, which may lead to reduced extraction efficiencies. With the increase of Span 80 concentration, the emulsion stability and Ce(III) transport capacity will increase, but too high levels of the surfactant cause the viscosity of the membrane to rise and make it difficult to transport Ce(III)-D2EHPA. According to the response surface obtained by the ANN model the best extraction efficiency (close to 100 %) is found at the intermediate concentration of Span 80 (2–4 wt. %), whereas higher concentrations of the surfactant result in the decrease of efficiency because of the increase in mass transfer resistance.

4.6.8 EFFECT OF VOLUME RATIO OF W/O EMULSION TO EXTERNAL PHASE

The volume ratio of the W/O emulsion to external phase plays an important role in the extraction efficiency because it alters the surface area, the external phase capacity and the stripping capacity of the emulsion phase. When the volume ratio is low enough, efficient use of the emulsion can result in good Ce(III) transport and high extraction efficiency. Volume ratio (quantity of water to product) greater than optimum can overload the emulsion system and adversely affect the effectiveness of carrier-mediated transport and internal stripping. The response surface obtained from ANN model suggests that higher ratio of emulsion loading is detrimental to the efficiency of extraction, as the extraction efficiency decreases with increasing volume ratio.

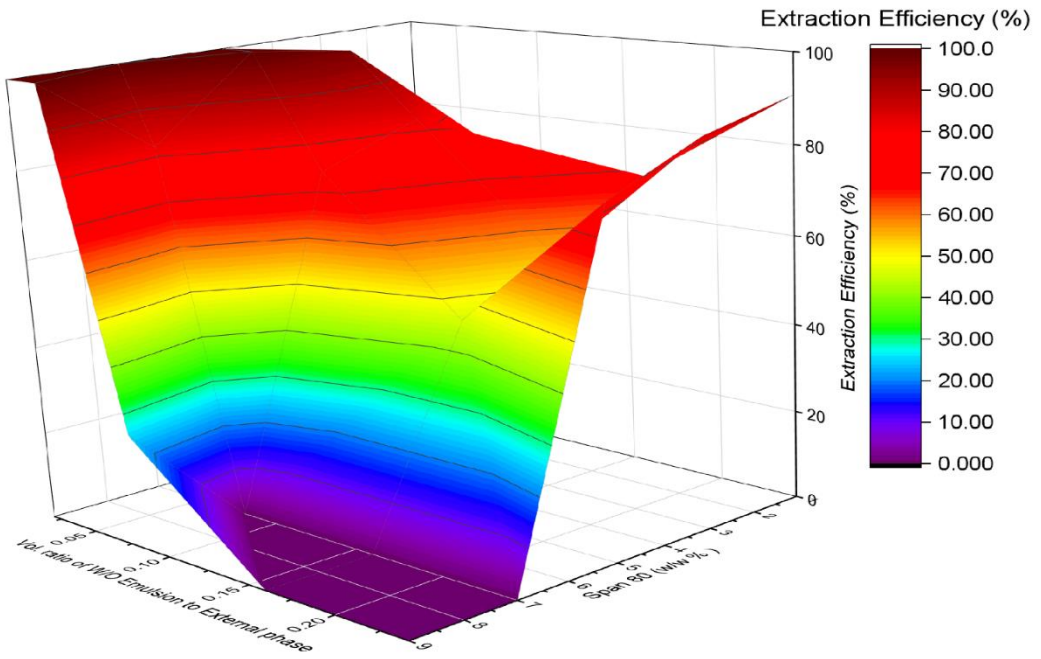

Figure 11: ANN-predicted 3D surface plot
showing the combined effect of Span 80 concentration (w/w %) and volume ratio of W/O emulsion to external phase on Ce (III) extraction efficiency (%).

4.6.9 COMBINED EFFECT OF SPAN 80 CONCENTRATION AND TREATMENT RATIO

The response surface predicted by ANN is nearly saddle-shaped, suggesting that there is strong interaction between the Span 80 concentration and ratio of volume of the W/O emulsion and external phase. The performance is highest around the intermediate Span 80 concentrations (2-4 wt.%) and low volume ratios and will be severely hampered at high concentrations and large volume ratios. This behavior is attributed to a combination of the emulsion stability, the viscosity of the membranes, and the utilization of the carriers: too little or too much amounts of Span 80 make for unstable emulsions, and too high volume ratios lead to an overloading of the emulsion system. The optimum operating region is therefore the area where the response surface is concave up, which corresponds to the highest Ce (III) extraction efficiency for the product to be both emulsion stable and maximizing the mass transfer of Ce (III).(Santiago et al., 2022b)

4.6.10 EFFECT OF INTERNAL PHASE CONCENTRATION (HNO_3)

Ce (III) extraction efficiency is greatly affected by the internal phase concentration of HNO_3, which affects the stripping of Ce (III) from the Ce–D2EHPA complex and the regeneration of the carrier in the emulsion membrane. It is observed from the graph that the extraction efficiency increases with the increase in the concentration of HNO_3 in the extraction process, especially in higher pH values of the feed, due to the availability of more H+ ions for stripping and the concentration gradient for continuous metal transport. However, the emulsion optimum is reached at the optimum concentration and higher concentrations of HNO_3 give only a small increase and can have a negative effect on emulsion stability.

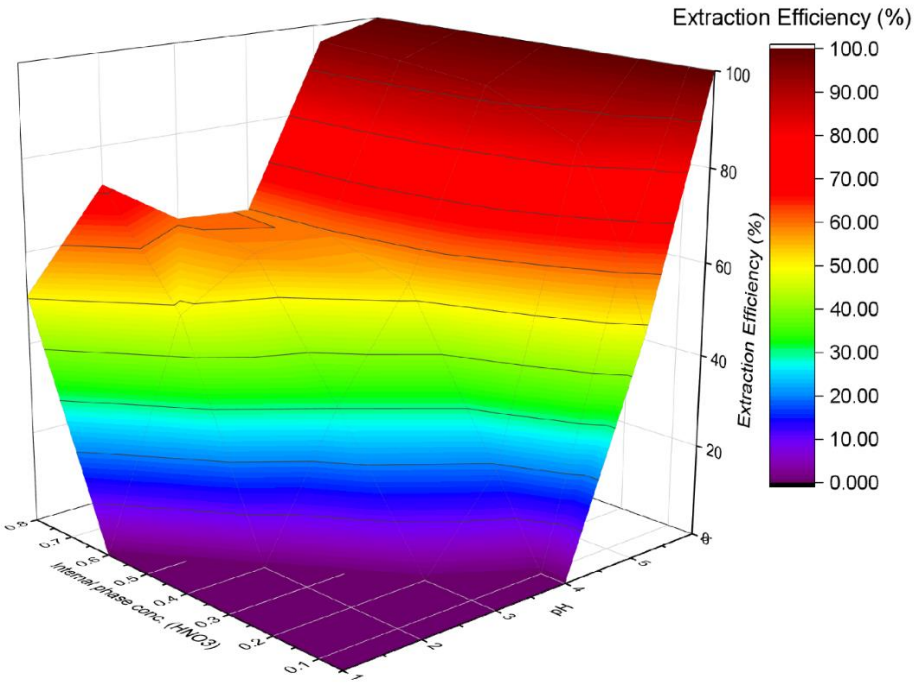

Figure 12: ANN-predicted 3D surface plot showing the combined effect of Internal Phase Concentration (HNO_3) and Feed Phase pH on Ce (III) extraction efficiency (%).

4.6.11 COMBINED EFFECT OF INTERNAL PHASE CONCENTRATION (HNO_3) AND FEED PHASE pH

The interaction between feed phase pH and internal phase HNO_3 concentration for the extraction efficiency of Ce (III) is synergistic and can be inferred from the combined response surface. As both variables increase, there is an improved extraction efficiency, with the best efficiencies being at high pH and moderate to high HNO_3 concentration. The positive effect of increasing HNO_3 concentration on the stripping and carrier regeneration increases when the extraction of Ce(III) into the membrane phase is favorable and thus increases with the increase in pH. The profile of the surface shows that for the best extraction, there should be very efficient extraction at the feed–membrane interface as well as very efficient stripping in the internal phase.

4.6.12 EFFECT OF EXTRACTION TIME

The extraction time has significant influence over efficiency of Ce (III) extraction as it determines the complexation, transportation and stripping inside the emulsion liquid membrane. The response surface indicates that the extraction efficiency rises sharply with the increasing amount of the contact time (due to the increased mass transfer of Ce (III) across the membrane) and then levels off at equilibrium. Apart from the optimum extraction time, there is no significant improvement, and even a decrease in extraction might be noticed, due to swelling of the emulsion, instability of the membrane or leakages, meaning that the optimum time for contact is necessary to obtain maximum extraction.(Dâas & Hamdaoui, 2010)

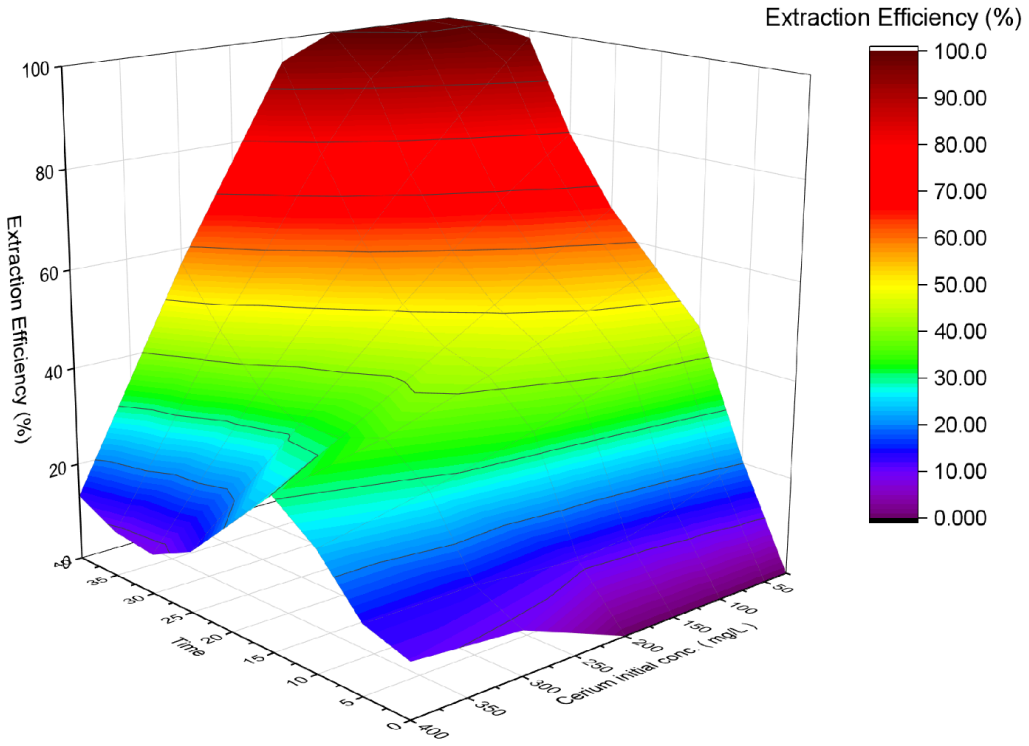

Figure 13: ANN-predicted 3D surface plot
showing the combined effect of extraction time and cerium initial concentration (mg/L)
on Ce (III) extraction efficiency (%).

4.6.13 COMBINED EFFECT OF EXTRACTION TIME AND Ce (III) INITIAL CONCENTRATION

The effect of the interaction between extraction time and initial Ce (III) concentration on the extraction efficiency can be shown from the response surface. The optimal Ce (III) concentration is around 0.01 M and the optimal extraction time is between 30 and 120 minutes, which is enough to complex and transport the Ce(III) but not so long to reach the saturation of the carrier. Extraction efficiency increases rapidly with time and saturates, while along the concentration axis it will increase to some optimum value and then decrease because of saturation of the carrier and limited stripping capabilities. The results showed that the extraction time must be optimized along with the removal of Ce (III) because increasing the extraction time will only improve the removal of Ce (III) within the capacity limit of the membrane system.(Lee et al., 2009)

4.7 OVERALL ANN MODEL PERFORMANCE

The overall performance of the ANN model shows that the developed network is able to represent the Ce (III)-ELM extraction system. The optimized network with 11 hidden layer neurons produced training R = 0.99435, validation R = 0.99082, test R = 0.97351, and overall R = 0.99082, with a minimum MSE of 26.145.

The results demonstrate high prediction accuracy and high generalization ability of the model in all data subsets. The extraction efficiency is high and the R value is high, this validates experimental and predicted extraction efficiencies to be well correlated. The small MSE value shows that the prediction error is small. All of these results indicate that ANN can be used as an efficient tool to model the non-linear behavior of Ce (III) extraction in an emulsion liquid membrane system.

The results are in agreement with other ELM systems, showing the importance of the process variables such as the pH of the feed phase, concentration of D2EHPA, concentration of Span80, concentration of HNO_3, stirring speed, and initial concentration of Ce(III) as reported in other ELM systems.(Frechen et al., 2008)

The present results are in agreement with the study of Tyagi et al. and Iqbal et al.(Kumar et al., 2021)who found that ANN is a powerful model tool for the separation processes of rare earth elements. ANN is useful for predicting the process performance and finding favorable operating conditions for ELM systems because experimental optimization can be time consuming and chemically intensive.

Table 4: Summary of ANN Model Performance

S. No.	Performance Parameter	Value
1.	ANN architecture	9–11–1
2.	Hidden layer neurons	11
3.	Output variable	Extraction efficiency (%)
4.	Correlation coefficient	$R \geq 0.99$
5.	Mean Squared Error	26.145
6.	Model performance	Excellent agreement between experimental and predicted values

4.7.1 Sensitivity Analysis: Relative Importance of Input Parameters

The magnitudes were obtained by following the Garson`s approach for determining the relative importance of each input parameter and are reported as percentage contribution to the total variance in the predicted extraction efficiency. The results are summarized as in Table 4.

Table 5: Relative importance of input parameters on Ce (III) extraction efficiency as determined by ANN sensitivity analysis.

Rank	Input Parameter	Relative Importance (%)
1	Feed phase pH	28.0
2	D2EHPA concentration (% w/w)	23.0
3	Stirring speed (rpm)	18.0
4	Span 80 concentration (% w/w)	12.0
5	HNO_3 (stripping agent) concentration (N)	10.0
6–9	Other parameters (treatment ratio, phase ratio, initial Ce (III) conc., extraction time)	9.0 (combined)

The sensitivity analysis shows that feed phase pH has the highest impact on extraction efficiency of Ce(III) (around 28% of the overall variability) because of the high influence on the D2EHPA-mediated cation-exchange mechanism. The second important parameter is D2EHPA concentration (23%), emphasizing the effect on metal transport that is caused by availability of the emulsifier, followed by stirring speed (18%), which determines the dispersion of the emulsion and the mass transfer. The concentration of Span 80 (12%) and HNO_3 (10%) also play significant roles in extraction due to the stability of the emulsion and the efficiency of the stripping process, respectively. All the other parameters, including the phase ratio, treatment ratio, initial Ce(III) concentration and extraction time, have comparatively small contributions, accounting for about 9% of the variability. The overall results have been validated and demonstrate that the ANN model can appropriately describe the physicochemical behavior of the ELM system.(Ma et al., 2015a)

4.7.2 Comparison with Published Literature (Table 16)

Results of the comparison showed that the 9–11–1 ANN model developed in this work can attain the competitive or better predictive performance compared to the previously published models for similar REE systems.

Table 6: Comparison of Present Study with Published ANN-Based Modeling Studies on Rare Earth Element Separation.

Study	Metal	Separation Method	ANN Architecture	R	MSE	Key Finding
Anitha & Singh [31]	La, Nd, Ce	Solvent Extraction	MLP (multiple)	0.987–0.997	—	First ANN application for REE solvent extraction equilibrium; demonstrated feasibility for lanthanide systems
Tyagi et al. [32]	Nd (III)	Liquid Membrane (D2EHPA)	MLP-GA hybrid	≥0.999	—	ANN-GA hybrid optimized Nd (III) ELM parameters; GA enhanced model convergence and accuracy
Iqbal et al. [33]	Dy (III)	Liquid Membrane (ELM)	MLP (LM algorithm)	≥0.999	—	ANN accurately predicted Dy (III) ELM performance; confirmed role of pH, D2EHPA, and Span 80 as primary parameters
Present Work	**Ce (III)**	**ELM (D2EHPA / Span 80 / HNO_3)**	**MLP (9–11–1, LM)**	**0.9908**	**26.145**	**First ANN model for Ce (III) ELM with 9 input variables; R^2=0.9817, RMSE≈5.11%; sensitivity analysis identified feed pH as dominant parameter (28%)**

The present ANN model for Ce(III)–ELM has a correlation coefficient (R = 0.9908) close to that of the best models reported in the literature for rare-earth-element liquid membrane systems.

Although Tyagi et al. and Iqbal et al. saw R = 0.999 using ANN-GA hybrid methods and smaller number of input variables (generally five to six as in similar studies), the present study used a larger number of input variables (nine variables versus normally five to six in similar studies), which made it more difficult to achieve very high R values. The MSE value reported in the present study is in the original units of extraction efficiency (%), and shows that the system is multi-variable. The study is the first ANN model applied to Ce (III) extraction by ELM developed by considering nine operating variables, giving a more comprehensive characterization of the process than the previous studies.(Kumar et al., 2021; Santiago et al., 2022a)

CHAPTER 5: CONCLUSION AND FUTURE SCOPE

5.1 CONCLUSION

The present dissertation aimed to investigate the modelling of the extraction of Ce (III) from aqueous solution using Artificial Neural Network (ANN) technology in which the extraction and stripping processes occur simultaneously in the form of an emulsion liquid membrane (ELM). The ELM system consisted of the external phase containing Ce (III), the organic phase containing D2EHPA as carrier and Span 80 as surfactant in kerosene, and the internal phase containing nitric acid; the transport of Ce (III) in the ELM system was carried out by complexation of Ce (III) with D2EHPA at the feed–membrane interface and subsequent stripping in the internal phase

The Levenberg–Marquardt algorithm was successfully used for developing a feed-forward backpropagation ANN model in MATLAB, where nine operating variables were used as inputs and extraction efficiency as the output. The optimized 9–11–1 architecture showed good and stable performance and a strong correlation with the experimental results, having an overall correlation coefficient R = 0.99082 (R^2 = 0.9817) and a low prediction error (MSE = 26.145, RMSE ≈ 5.11%). Close agreement for the predicted and experimental values for the three subsets (training, validation and test) confirms the reliability of the model, with sensitivity analysis showing that the feed phase pH (28%) and D2EHPA concentration (23%) were the most influential parameters.

The process behavior was successfully visualized using ANN generated three dimensional response surface plots and the interactions between the process parameters were identified. These surfaces allowed to test the effect of two operating parameters at the same time, showing synergic and antagonistic interactions, which could not be captured in a single parameter analysis and determining the best operating range of the process. Both extraction efficiency and concentration of surfactant and carrier were predicted to be high enough to approach 100% in moderately high pH with moderate stirring speeds and intermediate initial Ce (III) concentration. The trained model is able to predict the extraction efficiency for new operating conditions without any additional experiments within the considered range of studied conditions, which can save a significant amount of time, costs and experimental effort. In summary, the use of ELM technology combined with ANN modeling offers an efficient, selective and data-driven solution to recover Ce (III) from the aqueous solutions.

5.1.1 LIMITATIONS OF THE PRESENT STUDY

The model is an interpolation tool based on data points, the predictions of which are only valid within the range of parameters the model was trained on, and should not be extrapolated without further testing. The temperature was fixed and not considered as an input to the model, therefore isothermal conditions were considered. The size and quality of the training data and the consideration of a single-metal system limit the predictability, and selectivity under multi-metals industrial effluents is to be determined. Last but not least, the model was only tested in laboratory scale and scale-up to industrial scale adds more variables that need to be taken into consideration before deployment. These restrictions are stating the domain of applicability of the model, not reducing its scientific merits.

5.2 FUTURE SCOPE

Future works could involve using a larger and more diverse experimental dataset, as well as other performance metrics like average relative error and residual analysis, to further enhance the generalisation ability of the model. Other machine-learning methods like Support Vector Regression, Random Forest, Gradient Boosting and ANFIS can be used to compare the ANN approach and identify the most appropriate predictive instrument. The model can also be extended to multi-objective optimization using hybrid models, for instance, ANN coupled with genetic algorithm, particle swarm optimization or grey wolf optimizer, with experimental validation of the optimum conditions predicted by the model. Emulsion stability, phase separation, solvent recovery and economic feasibility scale-up studies should be performed in industrial applications and real effluents should be treated with the presence of competing metal ions. The use of advanced architectures, such as deep neural networks, LSTM networks for time-dependent behavior and Physics-Informed Neural Networks which incorporate the underlying transport and equilibrium equations, seems to be promising approaches for enhancing extrapolation capabilities. Based on the present study, a good foundation has been provided to further develop the ANN-assisted ELM processes for the recovery of valuable REs such as Ce(III) ions from the aqueous wastes.

REFERENCES

1. Abu Shmeis, R. M., Tarawneh, I. N., & Al-Majali, H. M. (2021). Removal of phenolic compounds from olive oil mill wastewater using kaolinite and iron oxide nanoparticles. *Desalination and Water Treatment*, *237*, 54–63. https://doi.org/10.5004/dwt.2021.27724
2. Ahmad, A., Priyadarshini, M., Yadav, S., Ghangrekar, M. M., & Surampalli, R. Y. (2022). The potential of biochar-based catalysts in advanced treatment technologies for efficacious removal of persistent organic pollutants from wastewater: A review. *Chemical Engineering Research and Design*, *187*, 470–496. https://doi.org/10.1016/j.cherd.2022.09.024
3. Allahkarami, E., & Rezai, B. (2021). A literature review of cerium recovery from different aqueous solutions. *Journal of Environmental Chemical Engineering*, *9*(1), 104956. https://doi.org/10.1016/j.jece.2020.104956
4. Dâas, A., & Hamdaoui, O. (2010). Extraction of anionic dye from aqueous solutions by emulsion liquid membrane. *Journal of Hazardous Materials*, *178*(1–3), 973–981. https://doi.org/10.1016/j.jhazmat.2010.02.033
5. Frechen, F. B., Schier, W., & Linden, C. (2008). Pre-treatment of municipal MBR applications. *Desalination*, *231*(1–3), 108–114. https://doi.org/10.1016/j.desal.2007.10.025
6. Gong, X., Shi, Q., Zhang, X., Li, J., Ping, G., Xu, H., Ding, H., & Li, G. (2023). Synergistic effects of PtFe/CeO2 catalysts afford high catalytic performance in selective hydrogenation of cinnamaldehyde. *Journal of Rare Earths*, *41*(2), 233–239. https://doi.org/10.1016/j.jre.2022.02.010
7. Himmelblau, D. M. (2008). Accounts of Experiences in the Application of Artificial Neural Networks in Chemical Engineering. *Industrial & Engineering Chemistry Research*, *47*(16), 5782–5796. https://doi.org/10.1021/ie800076s
8. Kamil, M. Z., Taleb-Berrouane, M., Khan, F., & Ahmed, S. (2019). Dynamic domino effect risk assessment using Petri-nets. *Process Safety and Environmental Protection*, *124*, 308–316. https://doi.org/10.1016/j.psep.2019.02.019
9. Kujawa, J., Al Gharabli, S., Szymczyk, A., Terzyk, A. P., Boncel, S., Knozowska, K., Li, G., & Kujawski, W. (2023a). On membrane-based approaches for rare earths separation and extraction – Recent developments. *Coordination Chemistry Reviews*, *493*, 215340. https://doi.org/10.1016/j.ccr.2023.215340
10. Kujawa, J., Al Gharabli, S., Szymczyk, A., Terzyk, A. P., Boncel, S., Knozowska, K., Li, G., & Kujawski, W. (2023b). On membrane-based approaches for rare earths separation and extraction – Recent developments. *Coordination Chemistry Reviews*, *493*, 215340. https://doi.org/10.1016/j.ccr.2023.215340
11. Kumar, V., Gupta, S., Kalra, J. S., & Patil, P. P. (2021). Improvement in quality of handmade paper materials by recycling of waste papers and PPE kits. *Materials Today: Proceedings*, *46*, 11274–11278. https://doi.org/10.1016/j.matpr.2021.03.487

12. Labas, M. D., Martín, C. A., & Cassano, A. E. (2005). Kinetics of bacteria disinfection with UV radiation in an absorbing and nutritious medium. *Chemical Engineering Journal*, *114*(1–3), 87–97. https://doi.org/10.1016/j.cej.2005.09.013
13. Laguel, S., & Samar, M. H. (2024a). Elimination of rare earth (neodymium (III)) from water by emulsion liquid membrane process using D2EHPA as a carrier in kerosene. *Desalination and Water Treatment*, *317*, 100214. https://doi.org/10.1016/j.dwt.2024.100214
14. Laguel, S., & Samar, M. H. (2024b). Elimination of rare earth (neodymium (III)) from water by emulsion liquid membrane process using D2EHPA as a carrier in kerosene. *Desalination and Water Treatment*, *317*, 100214. https://doi.org/10.1016/j.dwt.2024.100214
15. Lee, Y. G., Lee, Y. S., Jeon, J. J., Lee, S., Yang, D. R., Kim, I. S., & Kim, J. H. (2009). Artificial neural network model for optimizing operation of a seawater reverse osmosis desalination plant. *Desalination*, *247*(1–3), 180–189. https://doi.org/10.1016/j.desal.2008.12.023
16. Ma, L., Cao, L., & He, R. (2015a). Numerical study of pore structure effect on SO2–CaO reactions. *Chinese Journal of Chemical Engineering*, *23*(4), 652–658. https://doi.org/10.1016/j.cjche.2014.12.004
17. Ma, L., Cao, L., & He, R. (2015b). Numerical study of pore structure effect on SO2–CaO reactions. *Chinese Journal of Chemical Engineering*, *23*(4), 652–658. https://doi.org/10.1016/j.cjche.2014.12.004
18. Machado Cavalcanti, F., Emilia Kozonoe, C., André Pacheco, K., & Maria de Brito Alves, R. (2021). Application of Artificial Neural Networks to Chemical and Process Engineering. In *Deep Learning Applications*. IntechOpen. https://doi.org/10.5772/intechopen.96641
19. Mao, H., Zhou, D., Hashisho, Z., Wang, S., Chen, H., & Wang, H. (Helena). (2015). Constant power and constant temperature microwave regeneration of toluene and acetone loaded on microporous activated carbon from agricultural residue. *Journal of Industrial and Engineering Chemistry*, *21*, 516–525. https://doi.org/10.1016/j.jiec.2014.03.014
20. Mittal, S., Gupta, A., Srivastava, S., & Jain, M. (2021). Artificial Neural Network based modeling of the vacuum membrane distillation process: Effects of operating parameters on membrane fouling. *Chemical Engineering and Processing - Process Intensification*, *164*, 108403. https://doi.org/10.1016/j.cep.2021.108403
21. Ni'am, A. C., Wang, Y.-F., Chen, S.-W., Chang, G.-M., & You, S.-J. (2020). Simultaneous recovery of rare earth elements from waste permanent magnets (WPMs) leach liquor by solvent extraction and hollow fiber supported liquid membrane. *Chemical Engineering and Processing - Process Intensification*, *148*, 107831. https://doi.org/10.1016/j.cep.2020.107831
22. Perkins, C., Lichty, P., & Weimer, A. W. (2007). Determination of aerosol kinetics of thermal ZnO dissociation by thermogravimetry. *Chemical Engineering Science*, *62*(21), 5952–5962. https://doi.org/10.1016/j.ces.2007.06.039

23. Randhawa, N. S., Gharami, K., & Kumar, M. (2016). Leaching kinetics of spent nickel–cadmium battery in sulphuric acid. *Hydrometallurgy*, *165*, 191–198. https://doi.org/10.1016/j.hydromet.2015.09.011
24. Ronda, C. R., Jüstel, T., & Nikol, H. (1998). Rare earth phosphors: fundamentals and applications. *Journal of Alloys and Compounds*, *275–277*, 669–676. https://doi.org/10.1016/S0925-8388(98)00416-2
25. Santiago, V., Guerrero Zabala, F., Sanchez-Barra, A. J., Deisman, N., Chalaturnyk, R. J., Zhong, R., & Hurter, S. (2022a). Experimental investigation of the flow properties of layered coal-rock analogues. *Chemical Engineering Research and Design*, *186*, 685–700. https://doi.org/10.1016/j.cherd.2022.08.046
26. Santiago, V., Guerrero Zabala, F., Sanchez-Barra, A. J., Deisman, N., Chalaturnyk, R. J., Zhong, R., & Hurter, S. (2022b). Experimental investigation of the flow properties of layered coal-rock analogues. *Chemical Engineering Research and Design*, *186*, 685–700. https://doi.org/10.1016/j.cherd.2022.08.046